

Understanding the MiniBooNE and the muon and electron $g - 2$ anomalies with a light Z' and a second Higgs doublet

Waleed Abdallah,^{1,2,*} Raj Gandhi,^{1,†} and Samiran Roy^{1,3,‡}

¹*Harish-Chandra Research Institute, HBNI,*

Chhatnag Road, Jhansi, Allahabad 211019, India

²*Department of Mathematics, Faculty of Science, Cairo University, Giza 12613, Egypt*

³*Physical Research Laboratory, Ahmedabad - 380009, Gujarat, India*

Abstract

Two of the most widely studied extensions of the Standard Model (SM) are *a*) the addition of a new $U(1)$ symmetry to its existing gauge groups, and *b*) the expansion of its scalar sector to incorporate a second Higgs doublet. We show that when combined, they allow us to understand the electron-like event excess seen in the MiniBooNE (MB) experiment as well as account for the observed anomalous values of the muon magnetic moment. A light Z' associated with an additional $U(1)$ coupled to baryons and to the dark sector, with flavor non-universal couplings to leptons, in conjunction with a second Higgs doublet is capable of explaining the MB excess. The Z' obtains its mass from a dark singlet scalar, which mixes with the two Higgs doublets. Choosing benchmark parameter values, we show that $U(1)_{B-3L_\tau}$, which is anomaly-free, and $U(1)_B$, both provide (phenomenologically) equally good solutions to the excess. We also point out the other (anomaly-free) $U(1)$ choices that may be possible upon fuller exploration of the parameter space. We obtain very good matches to the energy and angular distributions for neutrinos and anti-neutrinos in MB. The extended Higgs sector has two light CP-even scalars, h' and H , and their masses and couplings are such that in principle, both contribute to help explain the MB excess as well as the present observed values of the muon and electron $g - 2$. We discuss the constraints on our model as well as future tests. Our work underlines the role that light scalars may play in understanding present-day low-energy anomalies. It also points to the possible existence of portals to the dark sector, *i.e.*, a light gauge boson field (Z') and a dark neutrino which mixes with the active neutrinos, as well as a dark sector light scalar which mixes with the extended Higgs sector.

Keywords: MiniBooNE excess, Muon and electron $g - 2$, $U(1)_B$, $U(1)_{B-3L_\tau}$

* Email Address: waleedabdallah@hri.res.in

† Email Address: raj@hri.res.in

‡ Email Address: samiran@prl.res.in

I. INTRODUCTION

The Standard Model (SM) of particle physics with its underlying framework of local gauge symmetries [1]¹ is a highly successful present-day theory. It explains, with impressive accuracy, an unprecedented range of experimental measurements over many decades in energy. In spite of its stellar success, however, the list of reasons as to why physics beyond the Standard Model (BSM) should exist is both long and compelling. Dark matter (DM) [4–8], the existence of which is extensively supported by a range of astronomical observations, is one of the strongest motivations for looking for new physics, because it is clear that none of the SM particles can contribute significantly to its share of the energy density of our universe. It is fair to say that despite assiduous efforts, practically no light has been shed so far on its particle properties.

The observed matter and anti-matter asymmetry in our universe [1, 9, 10] and the existence of small but non-zero neutrino mass differences [11–14], with masses widely different in magnitude from those of the charged leptons and quarks, as well as the existence of three families of quarks and leptons with a large mass hierarchy provide further grounds for the search for BSM physics.

A puzzling, and to a degree, unanticipated development in the effort to discover new physics is the lack of any definitive signals pointing to its presence at the Large Hadron Collider (LHC). Most notable among these is the absence (so far) of supersymmetry [15], which, arguably, has been the most popular model for BSM physics over the last three decades. This has led to renewed interest in the quest for BSM signals in other experiments, in settings as diverse as B-factories, rare decay searches, muon storage rings, matter-wave interferometers, pair-spectrometers for nuclear transitions and neutrino and DM detectors.

These efforts have not been disappointing. At the present time, there are several empirical results which appear to be anomalous at levels of statistical significance which invite, and in some cases, demand attention. Among them are observed discrepancies in *a*) the values of the anomalous magnetic moment of the muon [16, 17] and the electron [18], *b*) excesses in electron events in tension with muon neutrino disappearance data at short-baseline neutrino detectors [19], *c*) a significant excess in the signal versus background expectation in the

¹ For detailed pedagogical treatments see, for instance, [2, 3].

KOTO experiment [20] which searches for the decay of a neutral kaon to a neutral pion and a neutrino pair, *d*) discrepancies with SM predictions in observables related to B-decays [21], and finally, *e*) anomalies in the decay of excited states of Beryllium [22].

The possibility of connections between two or more of the sectors motivating the search for BSM physics has generated significant interest of late, and this work is also based on such a connection. For instance, the connection between neutrinos and the dark sector² pursued here has recently been discussed in [23–30].

For our purpose here, we note that if DM interacts with particles of the SM, its scattering must resemble neutral current interactions of neutrinos. This similarity is the reason why coherent elastic neutrino-nucleon scattering (CE ν NS) [31, 32] is a major background for next generation DM experiments looking to directly detect weakly interacting massive particles (WIMPs) [33]. This correspondence also underlies proposals and sensitivity studies for the direct detection of DM at fixed-target neutrino experiments (see, *e.g.* [34–42]) or even at much higher energies [43–46]. It follows, therefore, that persistent anomalous excesses in neutrino experiments should be scrutinized keeping in mind that they may be receiving contributions from dark sector particles scattering off SM particles via a mediating portal particle, which could be *i*) a vector, *ii*) a scalar or *iii*) a dark neutrino which mixes with the SM neutrinos.

In this work, we propose a solution to the electron-like event excess seen in the MiniBooNE (MB) experiment based on a new $U(1)$ symmetry associated with baryon number, mediated by a light new neutral gauge boson Z' , which couples either selectively or not at all to leptons. It also couples directly to particles in the dark sector and indirectly to neutrinos, via mixing. We do not propose a unique choice for the new gauge group insofar as its coupling to SM particles is concerned, but via benchmark parameters, show that both $U(1)_{B-3L_\tau}$ and $U(1)_B$ provide equally good solutions to the excess. We also indicate other (anomaly-free) choices that may be allowed once the parameter space is fully explored. The interaction (described in more detail below) which leads to the observed MB excess involves a dark neutrino, ν_d , mixed with the SM neutrinos, a SM Higgs sector expanded to include a second doublet, and a singlet (under the SM) scalar which couples to the SM fermions only via its mass mixing

² In what follows, the dark sector is assumed to comprise of particles which do not couple to SM fermions or gauge bosons, or do so extremely weakly and indirectly, *e.g.* via kinetic or mass mixings.

with the two Higgs doublet (2HD) sector³. While providing a very good fit to the MB data, this also accounts for the present observed value of the anomalous muon magnetic moment, without further embellishment or fine-tuning.

Section II discusses the observed excess in MB and the measured discrepant value of the anomalous muon and electron magnetic moments. Section III discusses our model, its motivations and Lagrangian, and presents the calculation of the process that leads to our explanation of the MB excess. Section IV A presents our results for MB and compares the neutrino and anti-neutrino energy and angular distributions obtained with the data. Sections IV B and IV C focus on the implications of our model for the anomalous magnetic moment of the muon and electron, respectively. Section V focuses on constraints on our work and discusses some possible future tests. Section VI qualitatively summarizes our results and conclusions.

II. THE MINIBOONE/LSND, THE MUON AND ELECTRON $g-2$ ANOMALIES

A. Event excesses in MiniBooNE and LSND

It is well-known that two neutrino experiments, MiniBooNE (MB) [48–53] and the Liquid Scintillator Neutrino Detector (LSND) (see [54], and references therein), have observed electron-like event excesses which have withstood scrutiny so far and which cannot be easily explained within the ambit of the SM. We summarize, in turn, the experiments, their results, and the efforts to explain them. Prior to proceeding, we note that while the discussion in this section covers both LSND and MB, given *a*) the fact that both see electron-like excesses and *b*) the many attempts to jointly explain them, our focus in the rest of the paper is the MB low-energy excess (LEE) and the anomalous magnetic moment of the muon. However, since the process chosen is, in principle, capable of giving the LSND final state, we also mention the implications for this in Section IV A, as well as discussing the consequences for the KARMEN experiment [55], which found a null result in its search for an LSND-like excess.

MB, at Fermilab, uses muon neutrino and anti-neutrino beams produced by 8 GeV protons hitting a beryllium target, with the fluxes peaking at around 600 MeV (ν_μ) and around

³ A more economical possibility, where only a singlet scalar with mass mixing to the SM Higgs is added, is precluded by very tight constraints on its fermionic couplings from a variety of experiments, see [47].

400 MeV ($\bar{\nu}_\mu$). The detector is a 40-foot diameter sphere containing 818 tons of pure mineral oil (CH_2) and is located 541 m from the target. Since 2002, the MB experiment has collected a total of 11.27×10^{20} POT in anti-neutrino mode and 18.75×10^{20} POT in neutrino mode. Quasi-elastic e -like event excesses of 560.6 ± 119.6 in the neutrino mode, and 79.3 ± 28.6 in the anti-neutrino mode, with an overall significance of 4.8σ have been established in the neutrino energy range $200 \text{ MeV} < E_\nu^{QE} < 1250 \text{ MeV}$. In terms of visible energy, E_{vis} , most of the excess is confined to the range $100 \text{ MeV} < E_{\text{vis}} < 700 \text{ MeV}$, with a somewhat forward angular distribution, and is referred to as the MB LEE. We note two points of relevance, *a*) that all major backgrounds are constrained by *in-situ* measurements, and *b*) that MB, being a mineral oil Cerenkov light detector, cannot distinguish photons from electrons in the final state. In addition, MB, under certain conditions (which we describe in more detail below) would also mis-identify an e^+e^- pair as a single electron or positron.

LSND was a detector with 167 tons of mineral oil, lightly doped with scintillator. Neutrino and anti-neutrino beams originating from π^- decay-in-flight (DIF) as well as μ decay-at-rest (DAR) were used. The main interaction was the inverse beta decay process, $\bar{\nu}_e + p \rightarrow e^+ + n$. The final state observed in the detector was the Cherenkov and scintillation light associated with the e^+ and the co-related and delayed scintillation light from the neutron capture on hydrogen, producing a 2.2 MeV γ . The experiment observed $87.9 \pm 22.4 \pm 6.0$ such events above expectations, at a significance of 3.8σ , over its run span from 1993 to 1998 at the Los Alamos Accelerator National Laboratory. Like MB, LSND was unable to discriminate a photon signal from those of e^+ , e^- or an e^+e^- pair.

B. Sterile neutrinos and other proposed new physics solutions of the MB and LSND anomalies

Perhaps the most widely discussed resolution of the MB and LSND excesses involves the presence of sterile neutrinos with mass-squared values of $\sim 1 \text{ eV}^2$, mixed with the SM neutrinos, leading to oscillations and $\bar{\nu}_e$ and ν_e appearance [52]. Support to the sterile hypothesis is lent by deficits in ν_e events in radioactive source experiments [56, 57] and in $\bar{\nu}_e$ reactor flux measurements [58–62]. Recent results from the reactor experiments, NEOS [63] and DANSS [64] also provide hints of oscillations involving sterile neutrinos. As other disappearance oscillation data sets and null results from multiple experiments have accumulated, however, this explanation for MB and LSND excesses has been subject to strongly increas-

ing tension with their conclusions. In particular, results from MINOS/MINOS+ [65] and IceCube [66] disappearance measurements constrain ν_μ mixing with a sterile neutrino very strongly, in conflict with the demands of the appearance hypothesis for MB and LSND. For recent global analyses and more detailed discussions, the reader is referred to [67–73]. Finally, the presence of a light sterile neutrino is also disfavoured by cosmological data [74, 75].

This growing tension and the tightening of constraints on the presence of sterile neutrinos has led to efforts to find non-oscillatory solutions to one or both of these excesses. Earlier attempts [76–79] have typically included a heavy sterile (*i.e.* dark) decaying neutrino which mixes with the SM active neutrinos. In proposals where the decay of the heavy neutrino is radiative [77, 78], there appears to be some conflict with either tight constraints on mixings and magnetic moments [80–87] or matching [79] the observed angular distribution of the visible light in MB. Other efforts invoking new physics include [88–91], which appear to be in tension with the conclusions of global analyses [68, 69, 71, 72]. Among more recent work we list [92, 93], which involve the production and fast decay of a heavy neutrino in MB, resulting in a collimated e^+e^- pair; [94] which depends on an altered ratio of single photon to π^0 events and [95] which invokes the production of a heavy neutrino in kaon decays in the proton beam target and its subsequent radiative decay. There have also been proposals [96, 97] which extend the decay scenario proposed in [76], originally proposed to explain LSND, and apply it to MB. Most recently [98, 99] discuss scalar mediated scenarios which also address the KOTO and the $g - 2$ anomalies in addition to MB, while [100] discusses it as well as a possible solution to $g - 2$ and the BaBar monophoton excess.

C. General constraint considerations relevant to new physics proposals for the MB LEE

While we discuss the constraints on our specific model in more detail later in this work, we list here some that are particularly important to most efforts to explain the MB LEE. Any explanation involving the production of dark sector particles in the target which then scatter elastically off the nucleons or electrons in the MB detector must confront the MB DM search results [41] which found no excess events in the off-target, *i.e.* beam dump mode. This result signals that when neutrino production was suppressed via charged pion absorption in the beam dump (*i.e.*, the target was removed) the excess disappeared. Another class of important constraints are those arising from neutrino-electron scattering measurements [101–106].

For a discussions of these constraints in the context of the MB LEE, see [107]. Finally, as we show below, a set of constraints important to any new physics proposal that involves a new coupling to baryons and a direct or indirect coupling to neutrinos originate from observations of neutral current neutrino-nucleon scattering at both low and high energies. At low energies, such a proposal must confront measurements such as those carried out by MB [108]. At high energies, the deep inelastic neutrino-nucleon cross sections [109–111] are well understood and tested by HERA data [112] all the way up to neutrino energies of 10^7 GeV, and these results must be complied with. Finally, a recent general treatment focussed on the MB LEE which brings out the difficulties and constraints associated with finding a solution to this anomaly may be found in [113].

D. The muon and electron $g - 2$ anomalies

The Lande g factor, and its deviation from the tree level value of 2, is one of the most precisely measured quantities in the SM. This also renders it an excellent probe for new physics. At the present time, there exists a long-standing and statistically significant discrepancy between its measurement [114, 115] and the theoretically predicted value, which involves contributions from quantum electrodynamics, quantum chromodynamics and electroweak theory [16, 17, 116–119]. Specifically, a 3.7σ muon $g - 2$ discrepancy has been found as follows [17]

$$\Delta a_\mu = a_\mu^{\text{meas}} - a_\mu^{\text{theory}} = (2.79 \pm 0.76) \times 10^{-9}. \quad (1)$$

Many proposals for new physics provide possible explanations for this discrepancy (For reviews and references, see [16, 116–118].). Our attempt in this work, details of which are provided in the sections to follow, is related to a class of possible solutions suggested by several authors [120–131] involving a light scalar with a mass in the sub-GeV range and a relatively weak coupling to muons.

Also, from the high precision measurement of the fine structure constant, a 2.4σ discrepancy has been recently found between the theoretical value and experimental measurement of the electron magnetic moment [18],

$$\Delta a_e = a_e^{\text{exp}} - a_e^{\text{theory}} = (-8.7 \pm 3.6) \times 10^{-13}. \quad (2)$$

III. THE MODEL, ITS MOTIVATIONS AND THE INTERACTION IN MINI-BOONE

A. Motivations for the choice of the additional $U(1)$

For reasons enumerated in the beginning of the previous section, one may legitimately assume that the SM is a highly successful low energy effective description of a more fundamental and complete theory. Effective field theories are not, in general, expected to satisfy the stringent requirements of renormalizability and anomaly cancellation, and yet the SM does satisfy these important criteria. One may choose to treat this as a curious accident, or one could adopt it as a guiding principle and impose ultra-violet (UV) completion and the freedom from anomalies as a desirable requirement [132] when considering a further $U(1)$ extension. We choose this approach for arriving at one of the benchmark choices we make here ($U(1)_{B-3L_\tau}$, below). From a phenomenological point of view, however, we find that a second option which does not satisfy these criteria, a $U(1)$ with gauged baryon number, works equally well for explaining the MB LEE and accommodating the muon and electron $g - 2$. This latter choice must, however, be supplemented by a set of heavy chiral fermions.

The global symmetries of the SM, namely, $U(1)_B, U(1)_{L_e}, U(1)_{L_\mu}$ and $U(1)_{L_\tau}$, provide possible signposts to an extension. These lead to three combinations which are anomaly-free and consequently do not require the addition of any new fermions, *i.e.*, $U(1)_{L_\mu-L_e}, U(1)_{L_e-L_\tau}$ and $U(1)_{L_\mu-L_\tau}$ [133–135]. In addition, if right-handed (RH) neutrinos are added to the SM particle spectrum, it can be shown [132, 136, 137] that $U(1)_{B-L} \times U(1)_{L_\mu-L_\tau} \times U(1)_{L_\mu-L_e}$ or any of its subgroups provide anomaly-free and UV complete options for adding a new $U(1)$ gauge boson to the SM. Noting that *a*) the necessary new physics to explain MB must couple neutrinos to baryons either directly or via mixing, (since the incoming beam is a ν_μ or a $\bar{\nu}_\mu$ and the target nucleus is CH_2) and, *b*) that a universal coupling to the quark generations ensures safety from flavor changing neutral currents (FCNCs), one is led to a class of symmetries, *i.e.* $B - r_\ell L_\ell$, with $r_\ell L_\ell = 3$, where the r_ℓ are real coefficients and $\ell = e, \mu, \tau$.

For several examples of this general class of possibilities, the phenomenology of and constraints on the associated boson have been studied in [106, 138–142]. They arise from beam dump, fixed target, collider, weak precision and neutrino experiments (for a com-

plete list, see [142] and references therein) which tightly restrict the gauge coupling and the mass of the new gauge boson. Additional constraints on electron couplings arise from neutrino electron elastic scattering experiments [102, 104, 105, 143]. Overall, one is led to the conclusion that it is very difficult to explain the MB LEE and simultaneously satisfy all constraints on a $U(1)$ if it couples to any significant degree to electrons. Based on this, possibilities, like $U(1)_{B-3/2(L_\mu+L_\tau)}$, $U(1)_{B-3L_\mu}$, and $U(1)_{B-3L_\tau}$, which, while also tightly constrained [137, 144], offer a little more room for accommodating new physics explanations. In our work, we have chosen to use $U(1)_{B-3L_\tau}$ [145–147] as an example, but it is possible that a fuller exploration of the possibilities available may yield other equivalent anomaly-free and UV complete options among the larger set $B - r_\ell L_\ell$ identified above.

As mentioned, $U(1)_B$ affords a phenomenologically equivalent alternative insofar as explaining the two anomalous results we focus on in our work. Gauging baryon number alone has been discussed extensively in the literature [25, 148–165]. A gauged $U(1)_B$, unlike the accidental SM symmetry combinations mentioned above, is not anomaly-free and must be treated as an effective theory with an UV cut-off, with new states entering at higher energies to make the theory consistent. A discussion of the necessary UV completions is outside the scope of our work and we refer the reader to the references above for examples of such models.

B. Some other considerations

The associated gauge boson (Z') for both our example gauge groups also couples to the dark sector. We note that there are observational reasons that hint towards a link that may exist between DM and baryons. These are the stability of both DM and protons on a timescale equal to or exceeding the age of the universe, and the empirically known but unexplained fact that the relic abundances of baryons are similar to those of DM up to a factor of ~ 5 [162]. The Z' in our work is a portal particle, coupled via $U(1)_{B-3L_\tau}$ (or $U(1)_B$) to the SM with a coupling g_B and to the dark sector via a coupling g_d .

Prior to providing details of the model and the interaction in MB in the two next sections, we discuss two important gauge invariant and renormalizeable terms associated with any new $U(1)$ that is linked to the SM, specifically to its $U(1)_Y$ hypercharge group. These involve kinetic [166] and mass mixings. After convenient field redefinitions (see, *e.g.*, [167]) they

enter the Lagrangian as

$$\mathcal{L} \supset e \epsilon Z'^\mu J_\mu^{\text{em}} + \frac{g}{c_W} \epsilon' Z'^\mu J_\mu^Z, \quad (3)$$

where Z and Z' are the weak neutral SM and new gauge bosons, J_μ^{em} and J_μ^Z the electromagnetic and Z currents, e is the usual electric charge, g is the weak gauge coupling, c_W is the cosine of the Weinberg angle, and ϵ and ϵ' parameterize the kinetic and mass mixings, respectively. In situations where ϵ (ϵ') is sizeable and has measurable phenomenological consequences for current or near-future experiments, the Z' is usually referred to as a “dark photon” (“dark Z ”). In general, even if one assumes that kinetic mixing vanishes at high energies, it re-appears via loop effects. Specifically, if there are i particles with mass M_i charged under both $U(1)_Y$ and the new $U(1)_{Z'}$ with couplings g_Y and $g_{Z'}$ respectively, kinetic mixing is generated at the loop level with a magnitude [166, 168]

$$\epsilon = \frac{g_Y g_{Z'}}{16\pi^2} \sum_i q_Y^i q_{Z'}^i \ln \frac{M_i^2}{\mu^2}, \quad (4)$$

where q_Y and $q_{Z'}$ are the respective charges and μ is a renormalization scale. In what follows, $g_{Z'} = g_{B-3L_\tau}$ or $g_{Z'} = g_B$ is constrained to be $\simeq 10^{-4}$ or smaller (see Fig. 6), rendering ϵ very small. This allows us to assume in what follows that the main decay modes of the Z' are to invisible particles of the dark sector. Finally, we note that kinetic mixing may also be naturally small below the electroweak scale, if in the full theory at high energy the $U(1)_{Z'}$ is actually embedded in a larger non-abelian gauge group [153].

The mass mixing ϵ' between the Z and Z' at tree level arises if there is a scalar which acquires a vacuum expectation value (vev) and is charged under both the $U(1)_Y$ and the $U(1)_{Z'}$. Given the fact that our model does not contain such a particle, and that $\epsilon' \propto m_{Z'}/m_Z$ [167] which is quite small, we also neglect the mass mixing term proportional to ϵ' in addition to ϵ . For completeness, we mention that constraints on the kinetic mixing of dark photons for low mass Z' are very severe, and arise from a large number of collider, neutrino, beam dump and other experiments; for a recent comprehensive discussion and list of references the reader is referred to [141, 169]. The physics of and constraints on a mass-mixed Z' are discussed in [167, 169, 170].

Finally, we extend the scalar sector of the SM by adding a second Higgs doublet, *i.e.*, the widely studied two Higgs doublet model (2HDM) [171, 172] and add *i*) a dark sector singlet scalar $\phi_{h'}$ which acquires a vev and gives mass to the Z' , and *ii*) a dark neutrino ν_d . The process we consider in order to explain the MB LEE involves a beam ν_μ , which

produces, (via mixing) a dark neutrino (ν_d), which is the mass eigenstate corresponding to ν_d . Also present in the final state are *i*) a recoiling nucleon (incoherent scattering) or nucleus (coherent scattering) and *ii*) a light scalar h' or H , which quickly decays to an e^+e^- pair. The scattering is mediated by Z' , as shown in (Fig. 1). RH neutrinos are introduced for the purpose of anomaly cancellation and for generating neutrino masses via the seesaw mechanism. Further details are provided in the sections below.

C. The Lagrangian of the model

As discussed above, the SM is extended by a second Higgs doublet, and either *i*) a $U(1)_{B-3L_\tau}$ gauge boson, coupled to baryons and the τ sector or *ii*) a $U(1)_B$ gauge boson coupled to baryon number alone with gauge coupling g_B ⁴, with no tree level couplings to the leptons of the SM. In both cases the coupling to the incoming muon neutrinos is indirectly generated via mixing with the dark neutrino ν_d , since the light new mediator Z' couples to it with coupling g_d . As may be seen from Table I, which lists the benchmark values we use below, we have assumed

$$g_B \ll g_d,$$

essentially dictated by constraints that we discuss in Section V A. Such a hierarchy of couplings could effectively arise, of course, from widely differing charges for the same gauge boson. Perhaps a more natural possibility [173] is to assume that the disparity originates in the mixing of two $U(1)$ gauge bosons Z_1 and Z_2 , with significantly different mass eigenvalues $m_1 \ll m_2$, with Z_1 coupling to only the dark sector and Z_2 coupling only to SM particles. The lighter mass eigenstate, a mixture of Z_1 and Z_2 , would then be effectively coupled to the SM with a coupling $g_B \sim g_d m_1^2/m_2^2$. A second possibility [174] leading to a $g_B \ll g_d$ involves an effective Z' , which has no tree level SM couplings but couples via non-renormalizable operators.

The SM Lagrangian is thus extended by the following terms to obtain \mathcal{L}_{tot} , the full Lagrangian of the extended theory,

⁴ In the remainder of our work, we use g_B as a generic notation for both the $U(1)_B$ coupling and/or the $U(1)_{B-3L_\tau}$ coupling for the most part, specifying g_{B-3L_τ} only when the context demands it, as, for instance, in Fig. 6 and Section V. We stress that in the numerical calculations, they correspond to the same values.

$$\mathcal{L}_{\text{tot}} \supset -\frac{1}{4}Z'_{\mu\nu}Z'^{\mu\nu} + \bar{\nu}_d\gamma^\mu(i\partial_\mu + g_d Z'_\mu)\nu_d + \mathcal{L}_q + \mathcal{L}_f - \mathcal{L}_Y^f - V + \mathcal{L}_S^{\text{Kin}} + \mathcal{L}_m, \quad (5)$$

where

$$\begin{aligned} \mathcal{L}_q &= \sum_q \frac{1}{3}g_B\bar{q}\gamma^\mu Z'_\mu q, \quad \mathcal{L}_f = \sum_f g_B q_f \bar{f}\gamma^\mu Z'_\mu f, \\ \mathcal{L}_Y^f &= \sqrt{2}\left[(Y_{ij}^u\tilde{\Phi}_1 + \tilde{Y}_{ij}^u\tilde{\Phi}_2)\bar{Q}_L^i u_R^j + (Y_{ij}^d\Phi_1 + \tilde{Y}_{ij}^d\Phi_2)\bar{Q}_L^i d_R^j + (Y_{ij}^e\Phi_1 + \tilde{Y}_{ij}^e\Phi_2)\bar{L}_L^i e_R^j + h.c.\right]. \end{aligned} \quad (6)$$

In the above, q runs over all the SM quarks, while f runs over the leptons with charge q_f to which Z' is coupled to, *e.g.* ν_τ , τ for our choice of $U(1)_{B-3L_\tau}$, and over none of the lepton generations for $U(1)_B$. In Eq. (7), Q_L, u_R, d_R are the left-handed (LH) quark doublets, RH up-type quarks and RH down-type quarks respectively. Similarly, L_L and e_R denote the LH SM lepton doublets and the RH charged leptons, respectively. Φ_1 and Φ_2 are the two doublets of the 2HDM, and Y_{ij} and \tilde{Y}_{ij} are the associated Yukawa coupling matrices.

Our approach with respect to the 2HDM in this section is similar to that followed in [131]. We write the scalar potential V in the Higgs basis $(\phi_h, \phi_H, \phi_{h'})$ [175, 176], with the λ_i denoting the usual set of quartic couplings

$$\begin{aligned} V &= \phi_h^\dagger \phi_h \left(\frac{\lambda_1}{2} \phi_h^\dagger \phi_h + \lambda_3 \phi_H^\dagger \phi_H + \mu_1 \right) + \phi_H^\dagger \phi_H \left(\frac{\lambda_2}{2} \phi_H^\dagger \phi_H + \mu_2 \right) + \lambda_4 (\phi_h^\dagger \phi_H)(\phi_H^\dagger \phi_h) \\ &+ \left\{ \left(\frac{\lambda_5}{2} \phi_h^\dagger \phi_H + \lambda_6 \phi_h^\dagger \phi_h + \lambda_7 \phi_H^\dagger \phi_H + \lambda'_5 \phi_{h'}^* \phi_{h'} - \mu_{12} \right) \phi_h^\dagger \phi_H + h.c. \right\} \\ &+ \phi_{h'}^* \phi_{h'} (\lambda'_2 \phi_{h'}^* \phi_{h'} + \lambda'_3 \phi_h^\dagger \phi_h + \lambda'_4 \phi_H^\dagger \phi_H + \mu'), \end{aligned} \quad (8)$$

where

$$\phi_h = \begin{pmatrix} H_1^+ \\ \frac{v+H_1^0+iG_1^0}{\sqrt{2}} \end{pmatrix} \equiv \cos\beta\Phi_1 + \sin\beta\Phi_2, \quad \phi_H = \begin{pmatrix} H_2^+ \\ \frac{H_2^0+iA^0}{\sqrt{2}} \end{pmatrix} \equiv -\sin\beta\Phi_1 + \cos\beta\Phi_2, \quad (9)$$

$$\phi_{h'} = \frac{v' + H_3^0 + iG_2^0}{\sqrt{2}}, \quad (10)$$

so that $v^2 = v_1^2 + v_2^2 \simeq (246 \text{ GeV})^2$ and $\tan\beta = v_2/v_1$, where $\langle\Phi_i\rangle = v_i/\sqrt{2}$ and $\langle\phi_{h'}\rangle = v'/\sqrt{2}$. Here, H_1^+, G_1^0 are the Goldstone bosons eaten up by the gauge bosons after the electroweak and $U(1)'$ symmetries are spontaneously broken. Therefore, the scalar kinetic term $\mathcal{L}_S^{\text{Kin}}$ can be written as

$$\mathcal{L}_S^{\text{Kin}} = \sum_{\mathcal{H}} (D_\mu^{\mathcal{H}} \phi_{\mathcal{H}})^\dagger D_\mu^{\mathcal{H}} \phi_{\mathcal{H}} \supset \frac{1}{2} g_d^2 (v' + H_3^0)^2 Z'_\mu Z'^\mu, \quad (11)$$

where

$$D_\mu^{h'} \phi_{h'} \equiv (\partial_\mu + i g_d Z'_\mu) \phi_{h'}. \quad (12)$$

Hence, the $Z'-H_3^0-Z'$ coupling is given by

$$G_{Z'Z'H_3^0} = i \frac{2m_{Z'}^2}{v'}, \quad (13)$$

where $m_{Z'}^2 = g_d^2 v'^2$. The mass matrix of the neutral CP-even Higgses in the basis: (H_1^0, H_2^0, H_3^0) is given by

$$m_{\mathcal{H}}^2 = \begin{pmatrix} \lambda_1 v^2 & \lambda_6 v^2 & \lambda'_3 v v' \\ \lambda_6 v^2 & \bar{m}_H^2 & \lambda'_5 v v' \\ \lambda'_3 v v' & \lambda'_5 v v' & 2\lambda'_2 v'^2 \end{pmatrix}, \quad (14)$$

where $\bar{m}_H^2 = \mu_2 + (\lambda_3 + \lambda_4 + \lambda_5)v^2/2 + \lambda'_4 v'^2/2$. Here, we have used the following minimization conditions of the scalar potential V ,

$$\mu_1 = -\frac{1}{2}(\lambda_1 v^2 + \lambda'_3 v'^2), \quad (15)$$

$$\mu_{12} = \frac{1}{2}(\lambda_6 v^2 + \lambda'_5 v'^2), \quad (16)$$

$$\mu' = -\lambda'_2 v'^2 - \frac{\lambda'_3 v^2}{2}. \quad (17)$$

The mass matrix of the neutral CP-even Higgses $m_{\mathcal{H}}^2$ is diagonalized by $Z^{\mathcal{H}}$ as follows (see appendix A):

$$Z^{\mathcal{H}} m_{\mathcal{H}}^2 (Z^{\mathcal{H}})^T = (m_{\mathcal{H}}^2)^{\text{diag}}, \quad \text{with} \quad H_i^0 = \sum_j Z_{ji}^{\mathcal{H}} h_j, \quad (18)$$

where $(h_1, h_2, h_3) = (h, H, h')$ are the mass eigenstates, and $H_1^0 \approx h$ is the SM-like Higgs in the alignment limit (*i.e.*, $\lambda_6 \sim 0 \sim \lambda'_3$) assumed here. The masses of the CP-even physical Higgs states (h, H, h') are given by

$$m_{h,H,h'}^2 \simeq \left\{ \lambda_1 v^2, \frac{1}{2} \left(\bar{m}_H^2 + 2\lambda'_2 v'^2 \pm \sqrt{(\bar{m}_H^2 - 2\lambda'_2 v'^2)^2 + 4(\lambda'_5 v v')^2} \right) \right\}. \quad (19)$$

Also, in the present model, the charged and CP-odd Higgs masses, respectively, are given by

$$m_{H^\pm}^2 = \frac{1}{2} (2\mu_2 + \lambda_3 v^2 + \lambda'_4 v'^2), \quad (20)$$

$$m_A^2 = \frac{1}{2} (2\mu_2 + (\lambda_3 + \lambda_4 - \lambda_5) v^2 + \lambda'_4 v'^2). \quad (21)$$

Our explanation of the muon and electron $g-2$ draws upon contributions from two light scalars, h' and H , leading to $m_H^2, m_{h'}^2 \ll m_{H^\pm}^2, m_A^2$. As discussed in a later section, electroweak precision measurements, expressed in terms of oblique parameters, lead to a mass

hierarchy $m_A \sim m_{H^\pm} \gg m_H$. In addition, collider constraints (discussed in a later section below) set a lower bound on m_{H^\pm} , requiring it to be comfortably above ~ 110 GeV. For our purpose, we assume $m_{H^\pm}^2 \simeq m_A^2$. They do not play an essential role in our scenario, and we have checked that contributions made by them to the muon and electron $g - 2$ are negligibly small. The necessary closeness in mass then implies $\lambda_4 \simeq \lambda_5$, leading to $m_{H^\pm}^2 = m_A^2 \simeq -v^2 \lambda_5$. Perturbativity ($|\lambda_5| \lesssim \sqrt{4\pi}$) then imposes an upper bound on these masses, $m_{H^\pm} = m_A \lesssim 460$ GeV, with m_H thus restricted to be \sim GeV or less [131].

As we discuss in a later section, LEP allows us to obtain a lower bound on the charged Higgs, *i.e.* $m_{H^\pm} \simeq v\sqrt{|\lambda_5|} \geq 110$ GeV. This upper bound can be then translated to $|\lambda_5| \geq 0.2$. This is relatively insensitive to mass in the low mass region, *i.e.* $m_H \leq 1$ GeV.

In the Higgs basis the Lagrangian \mathcal{L}_Y^f can be written as follows

$$\mathcal{L}_Y^f = \sqrt{2} \left[(X_{ij}^u \tilde{\phi}_h + \bar{X}_{ij}^u \tilde{\phi}_H) \bar{Q}_L^i u_R^j + (X_{ij}^d \phi_h + \bar{X}_{ij}^d \phi_H) \bar{Q}_L^i d_R^j + (X_{ij}^e \phi_h + \bar{X}_{ij}^e \phi_H) \bar{L}_L^i e_R^j + h.c. \right], \quad (22)$$

where

$$X_{ij}^k = Y_{ij}^k \cos \beta + \tilde{Y}_{ij}^k \sin \beta, \quad (23)$$

$$\bar{X}_{ij}^k = -Y_{ij}^k \sin \beta + \tilde{Y}_{ij}^k \cos \beta. \quad (24)$$

We emphasize that X_{ij}^k and \bar{X}_{ij}^k are independent Yukawa matrices. Moreover, the fermion masses receive contributions only from X_{ij}^k , since in the Higgs basis only ϕ_h acquires a non-zero vev. This leads to $X^k = \mathcal{M}_k/v$, where \mathcal{M}_k are the fermion mass matrices. Hereafter, we work in a basis in which the fermion mass matrices are real and diagonal, where $U_k \mathcal{M}_k V_k^\dagger = m_k^{\text{diag}}$ are their bi-unitary transformations. In this basis, in general, \bar{X}_{ij}^k are free parameters and non-diagonal matrices.

From the leptonic Lagrangian \mathcal{L}_Y^ℓ , their interactions with the physical scalar states are given by

$$\mathcal{L}_Y^\ell = \sum_{\ell=e,\mu,\tau} [X_{ij}^\ell h + \bar{X}_{ij}^\ell (Z_{32}^\mathcal{H} h' + Z_{22}^\mathcal{H} H)] \bar{\ell}_L^i \ell_R^j + h.c., \quad (25)$$

one finds the following coupling strengths of the scalars h, h', H with a lepton pair, respectively:

$$y_\ell^h = \frac{m_\ell}{v}, \quad y_\ell^{h'} = y_\ell^\ell Z_{32}^\mathcal{H} = y_\ell^\ell \sin \delta, \quad y_\ell^H = y_\ell^\ell Z_{22}^\mathcal{H} = y_\ell^\ell \cos \delta, \quad (26)$$

where $\text{diag}\{m_e, m_\mu, m_\tau\} = U_\ell \mathcal{M}_\ell V_\ell^\dagger$ and δ is the scalar mixing angle between the mass eigenstates (H, h') and the gauge eigenstates (H_2^0, H_3^0) . In the above, we work in the mass

basis where the diagonal elements of the rotated $\bar{X}_{ij}^\ell = \text{diag}\{y^e, y^\mu, y^\tau\}$ and to avoid most of flavor violating processes and explain electron $g - 2$ simultaneously, we have chosen all off-diagonal elements to be zero except $y^{e\tau}$ and $y^{\tau e}$, as we discuss in Section IV C. Additionally, the quark \bar{X}_{ij}^k are assumed to be very small to suppress flavor violating processes. An example of an ansatz that can achieve such suppression is discussed in [177].

Finally, \mathcal{L}_m represents mass terms for the SM fermions, weak gauge bosons and the neutrinos. The full neutrino mass matrix contains mass terms for both the SM neutrinos and the additional ones we introduce, since the masses are linked to each other at the Lagrangian level. In addition to a LH ν_d , we have a RH partner (N_R^4) to cancel the $[U(1)']^3$ anomaly in the dark sector, as well as three RH neutrinos ($N_R^i, i = 1, 2, 3$) to achieve the usual SM anomaly cancellation. We further assume that the mass eigenstates of the RH neutrinos are large (to induce the see-saw mechanism) and can be integrated out. Thus at the low energies of interest to us here, one is left with a 4×4 mixing matrix U , which connects the flavor states e, μ, τ, d to the mass eigenstates ν_1, ν_2, ν_3 and ν_4 , and U_{PMNS} , the usual SM lepton sector mixing matrix is a 3×3 sub-matrix of U .

D. The interaction in MiniBooNE

As mentioned above, the dark neutrino (ν_d) mixes with the standard massive neutrinos. Writing the interaction term in the mass basis, we have

$$\mathcal{L}_{\text{int}} = -g_d \sum_{i,j=1}^4 U_{di}^* U_{dj} \bar{\nu}_i \gamma^\mu Z'_\mu \frac{(1 - \gamma_5)}{2} \nu_j. \quad (27)$$

The assumed value of the mass of the ν_4 plays a somewhat secondary role in our calculation, and we comment here on its dependence, which arises primarily from kinematic considerations. Varying the mass within a range allowed by existing constraints does not affect the results in a qualitative manner. The benchmark value (see Table I) for its mass assumed in what follows is ~ 50 MeV, hence it will not be produced in pion decay. Thus, in our model, the MB beam primarily consists of ν_μ produced via pion decay as the superposition of three mass eigenstates. The relevant process leading to an excess proceeds via the new Z' , producing a collimated e^+e^- pair via the light scalar (h') decay. As part of the final state, a ν_4 kinematically accessible for the MB neutrino beam energy is also produced, making it proportional to $|U_{\mu 4}|^2$, as shown in the Fig. 1. In what follows, we have assumed that the

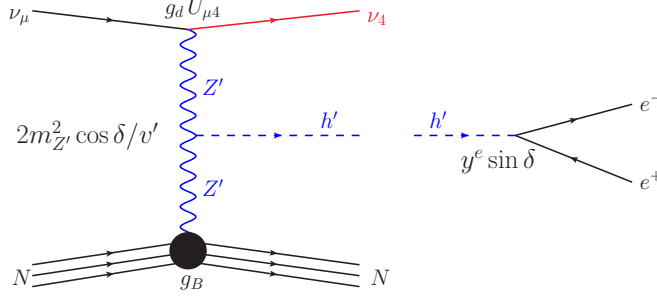


FIG. 1: Feynman diagram of the scattering process in our model which leads to the excess in MB. Note that H also contributes via the same diagram.

ν_4 does not decay visibly in MB after production. The Z' couples to quarks via its coupling to baryon number, and consequently to nucleons, denoted below by N . The on-shell matrix elements of the new Z' neutral currents take the form

$$\langle N(k') | J_{Z'}^\mu | N(k) \rangle = g_B \bar{u}(k') \Gamma_{Z'}^\mu(k' - k) u(k),$$

where, k and k' are the initial and final nucleon momenta, and

$$\Gamma_{Z'}^\mu(q) = \gamma^\mu F_V^1(q^2) + \frac{i}{2m_N} \sigma^{\mu\nu} q_\nu F_V^2(q^2). \quad (28)$$

The isoscalar form factors $F_V^1(q^2)$ and $F_V^2(q^2)$ for the nucleon are given by [178]

$$\frac{F_V^1(q^2)}{F_D(q^2)} = 1 - \frac{q^2(a_p + a_n)}{4m_N^2 - q^2}, \quad \frac{F_V^2(q^2)}{F_D(q^2)} = \frac{4m_N^2(a_p + a_n)}{4m_N^2 - q^2}, \quad (29)$$

where $m_N = 0.938$ GeV, $F_D(q^2) = (1 - q^2/0.71 \text{ GeV}^2)^{-2}$, $a_p \approx 1.79$ and $a_n \approx -1.91$ are coefficients related to the magnetic moments of the proton and neutron, respectively.

To compute the total differential cross section, we consider both the incoherent and coherent contributions in the production of h' , as shown in Fig. 1. The total differential cross section, for the target in MB, *i.e.*, CH_2 , is given by

$$\left(\frac{d\sigma}{dE_{h'}} \right)_{\text{CH}_2} = \underbrace{14 \times \left(\frac{d\sigma}{dE_{h'}} \right)}_{\text{incoherent}} + \underbrace{144 \times \exp(2b(k' - k)^2) \left(\frac{d\sigma}{dE_{h'}} \right)}_{\text{coherent}}. \quad (30)$$

For the incoherent process, we have multiplied the single nucleon cross section by the total number of the nucleons present in CH_2 *i.e.*, 14. In the coherent process the entire carbon nucleus (C^{12}) contributes in the process and the contribution is large when the momentum transfer is small, *i.e.* $q^2 = (k' - k)^2 \sim 0$. As q^2 increases, the coherent contributions are

reduced significantly. This is implemented by the form factor $\exp(2b(k' - k)^2)$ [179], where b is a numerical parameter, which for C^{12} , has been chosen to be 25 GeV^{-2} [31, 179].

We have used Eq. (30) to calculate the total number of h' produced in the final state. Once h' is produced, it decays promptly to an e^+e^- pair, its lifetime being decided by its coupling to electrons. Neglecting the mass of the electron, the lifetime of h' is given by

$$\tau_{h'} = \frac{8\pi}{(y_e^{h'})^2 m_{h'}}. \quad (31)$$

For our benchmark parameter values, the lifetime of h' is 3.5×10^{-13} seconds. We note that MB is not able to distinguish an e^+e^- pair from a single electron [180, 181] if $m_{\text{track}} < 30 \text{ MeV}$, where

$$m_{\text{track}} \equiv \sqrt{2E_1 E_2 (1 - \cos \theta_{12})}. \quad (32)$$

Here E_1 and E_2 are the track energies and θ_{12} is the angle between two tracks. Since we have chosen the mass of h' to be 23 MeV , the m_{track} produced by h' decay is always less than 30 MeV . Hence, the decay of h' to an e^+e^- pair mimics the single electron charged current quasi-elastic (CCQE) signal in the detector. We note that H can also contribute to the MB signal, since it can be produced in the final state and subsequently decay promptly to an e^+e^- pair. If the opening angle of the two electrons is less than 8° or one of electrons has energy less than 30 MeV , it would add to the signal. We find that only a fraction ($\sim 10 - 15\%$) of the total number of the H produced satisfy these criteria. Further suppression are provided by kinematics, since its mass is higher than that of h' , and by $\sin^2 \delta$. Hence, the contribution of H to the MB events is small. Additionally, we have checked that the production of two h' s, two H s or $h'H$ via the quartic couplings to Z' is suppressed compared to single h' production in the final state.

Our results are presented in the next section⁵.

IV. RESULTS

In this section we present the results of our numerical calculations, using the cross section for the process and the model described in Section III.

⁵ The results we present have been computed using our own code, and checked subsequently by implementing the present model in SARAH [182, 183] and by using MadGraph5_aMC@NLO [184].

A. Results for MiniBooNE and implications for LSND and KARMEN

Fig. 2 shows, in each of the 4 panels, the data points⁶, SM backgrounds and the prediction of our model (blue solid line) in each bin. Also shown (black dashed line) is the oscillation best fit. The left panel plots show the distribution of the measured visible energy, E_{vis} , plotted against the events for neutrinos (top) and anti-neutrinos (bottom). For our model, E_{vis} corresponds to $E_{h'}$. The right panels show the corresponding angular distributions for the emitted light. The benchmark parameter values used to obtain the fit from our model are shown in Table I. The plots have been prepared using fluxes, efficiencies POT exposures and other relevant information from [52, 53] and references therein. We see that very good fits to the data are obtained both for energy and angular distributions. (The data points show only statistical uncertainties.). We have assumed a 15% systematic uncertainty for our calculations. These errors are represented by the blue bands in the figures.

m_{ν_4} (MeV)	$m_{Z'}$ (MeV)	$m_{h'}$ (MeV)	m_H (MeV)	$ U_{\mu 4} ^2$	g_B	g_d	$\sin \delta$	$y_{e(\mu)}^{h'} = y^{e(\mu)} \sin \delta$	$y_{e(\mu)}^H = y^{e(\mu)} \cos \delta$	$ y^{e\tau} y^{\tau e} $
50	800	23	106	2.6×10^{-5}	3×10^{-4}	2.85	0.28	$0.45(1.8) \times 10^{-4}$	$1.5(6.0) \times 10^{-4}$	5.6×10^{-7}

TABLE I: Benchmark parameter values used for event generation in MB and for calculating the muon and electron $g - 2$.

As mentioned earlier, the LSND observations measure the visible energy from the Cerenkov and scintillation light of an assumed electron-like event, as well as the 2.2 MeV photon resulting from coincident neutron capture on hydrogen. In our model, this corresponds to the scattering diagrams in Fig. 1 where the target is a neutron in the Carbon nucleus. Unlike the case of MB above, where both coherent and incoherent processes contribute to the total cross section, the LSND cross section we have used includes only an incoherent contribution. Using the same benchmark parameters as were used to generate the MB results, as well as all pertinent information on fluxes, efficiencies, POT etc from [54, 185–188], we find a very small excess (1 – 2 events, from the DIF flux only), compared to the much larger observed excess reported by LSND [54]. We note that our calculations do not include

⁶ Note that the latest data for the neutrino mode, corresponding to 18.75×10^{20} POT, as detailed in [53] have been used in our fit.

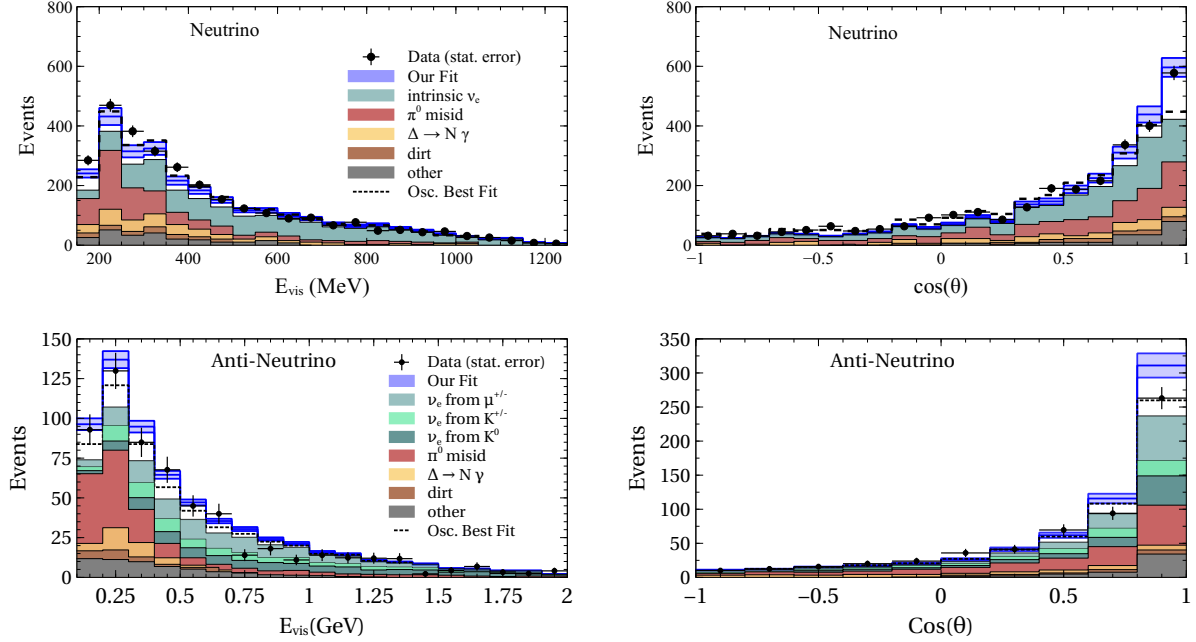


FIG. 2: The MB electron-like events (backgrounds and signal) from [52, 53], versus the visible energy E_{vis} and versus the cosine of the emitted angle of the light, for neutrino (top) and anti-neutrino (bottom) runs. Data points show statistical errors, whereas the blue band shows (estimated) systematic errors. The blue solid line is the prediction of our model. The parameter values used in calculating it are shown in Table I.

effects arising from final state interactions or other considerations like nuclear screening or multiple scattering inside the nucleus, which could play a role at the LSND energies [189]. The KARMEN experiment similarly employed a mineral oil detection medium, but was less than a third of the size of LSND. It did not have a significant DIF flux, but had similar incoming proton energy and efficiencies. Unlike LSND, it saw no evidence of an excess. A simple scaling estimate using our LSND result gives ~ 0 events in KARMEN using our model, which is consistent with their null result.

B. Muon anomalous magnetic moment

The one-loop contribution of a scalar ϕ (as shown in Fig. 3) to the muon anomalous magnetic dipole moment is given by [190, 191]

$$\Delta a_\mu^\phi = \frac{(y_\mu^\phi)^2}{8\pi^2} \int_0^1 dx \frac{(1-x)^2(1+x)}{(1-x)^2 + x r_\phi^2}, \quad (33)$$

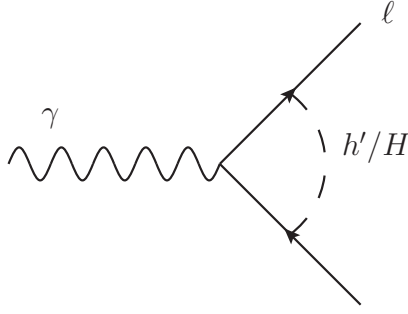


FIG. 3: One-loop contribution to lepton anomalous magnetic moments from the neutral scalars h' and H .

where $r_\phi = m_\phi/m_\mu$, and $\phi = h', H$. y_μ^ϕ is the coupling strength of the scalar ϕ with the muon pair, which is defined in Eq. (26).

In our scenario, both h' and H have comparable contributions to the muon anomalous magnetic moment given that they have light masses ≤ 1 GeV [129, 130]. In Fig. 4, we show the relative contributions of h' and H to Δa_μ as a function of the scalar mixing angle δ . The blue dashed and red dotted lines correspond to the muon anomalous magnetic moment contributions of H and h' (Δa_μ^H and $\Delta a_\mu^{h'}$), respectively, while the green solid line refers to their sum ($\Delta a_\mu^H + \Delta a_\mu^{h'}$). In addition, the horizontal yellow band indicates the 3.7σ muon $g-2$ discrepancy: $\Delta a_\mu = (2.79 \pm 0.76) \times 10^{-9}$ [17] and the black star denotes our benchmark in Table I. We note that in this figure $m_{h'}$, m_H are fixed to fit the MB measurements, as discussed in the previous section. We see that both h' and H have reasonable and comparable contributions to the total muon anomalous magnetic moment Δa_μ and their ratio $\Delta a_\mu^{h'}/\Delta a_\mu^H \sim \tan^2 \delta$. Although in our scenario are fixed $m_{h'}$ and m_H to fit the MB measurements, in a more general situation y^μ and the angle δ are still free parameters and one can fix them to fit the central value for Δa_μ .

For a suitably selected combination of y^μ and δ ($y^\mu = 6.3 \times 10^{-4}$ and $\sin \delta = 0.28$), our benchmark (denoted by the black star) is situated in the experimental allowed region (yellow band), close to the central value for Δa_μ ($= 2.74 \times 10^{-9}$). For our benchmark, it is clearly seen that while the total muon anomalous magnetic moment Δa_μ is dominated by the H contribution Δa_μ^H (blue dashed line), the h' contribution (red dotted line) is 18% of Δa_μ , which is not negligible. The constraints on y_μ^ϕ ($\phi = h', H$) are shown in Fig. 9. We see that both $y_\mu^{h'}$ and y_μ^H sit in the experimentally allowed region of the current constraint of

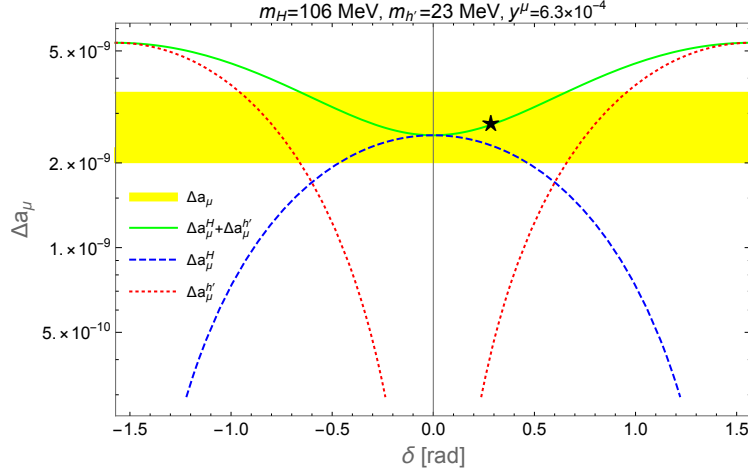


FIG. 4: Muon anomalous magnetic moment versus the scalar mixing angle δ , along with our benchmark in Table I denoted by the black star.

BaBar [192] and the future sensitivity of Belle-II [193].

C. Electron anomalous magnetic moment

In this sub-section, we consider the one-loop contribution of a light scalar ϕ (h' , H in our model) to the electron anomalous magnetic moment which is given by [190, 191]

$$\Delta a_e^\phi = \sum_{\ell=e,\mu,\tau} \frac{y_{e\ell}^\phi y_{\ell e}^\phi}{8\pi^2} \int_0^1 dx \frac{(1-x)^2(r_\ell + x)}{(1-x)^2 + x r_\phi^2 + (1-x)(r_\ell^2 - 1)}, \quad (34)$$

where $r_X = m_X/m_e$ and $y_{ee}^\phi = y_e^\phi$ is the coupling strength of the scalar ϕ with the electron pair, as defined in Eq. (26). To evade the $\text{BR}(\mu \rightarrow e\gamma)$ and $\text{BR}(\tau \rightarrow \mu\gamma)$ experimental upper bounds [194, 195] and explain the electron $g - 2$ anomaly, hereafter, we have chosen $y_{\mu e(e\mu)}^\phi$ and $y_{\mu\tau(\tau\mu)}^\phi$ to be sufficiently tiny and the product $y_{\tau e}^\phi y_{e\tau}^\phi$ is negative. Overall, Δa_e gets a positive contribution due to the non-vanishing Yukawa couplings y_e^ϕ which are fixed to fit the MB measurements, as discussed in section IV A. Also, it gets a negative contribution from τ inside the loop, since the product $y_{\tau e}^\phi y_{e\tau}^\phi$ is negative and is essentially a free parameter in our scenario. Thus, one can choose the absolute value of this product to fit the central value of Δa_e . Note that $y_{\tau e(e\tau)}^{h'} = y^{\tau e(e\tau)} \sin \delta$ and $y_{\tau e(e\tau)}^H = y^{\tau e(e\tau)} \cos \delta$.

In our scenario, as mentioned earlier, h' and H have light masses and consequently both contribute to the electron $g - 2$ anomaly, Δa_e . In Fig. 5, we show the relative contributions of h' and H to Δa_e versus the absolute product $|y^{e\tau} y^{\tau e}|$. The blue dashed and red dotted lines correspond to the electron anomalous magnetic moment contributions of H and h'

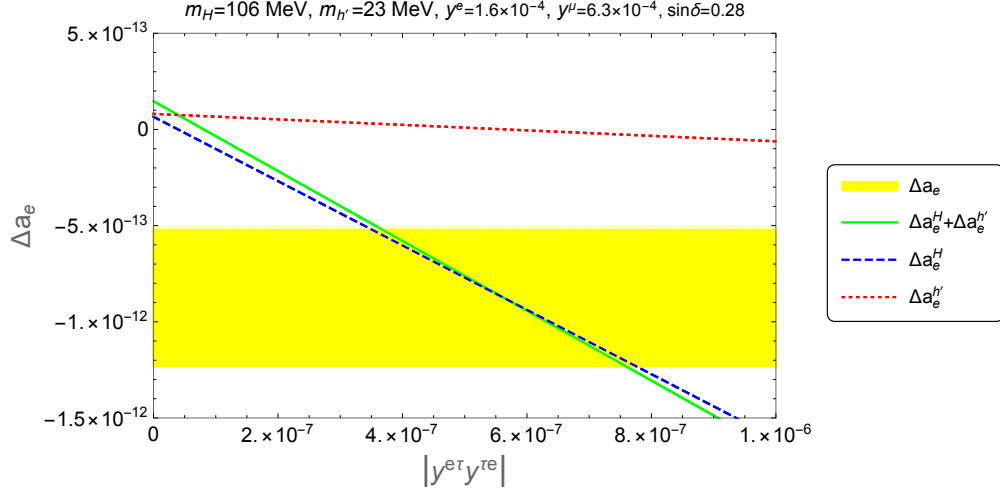


FIG. 5: Electron anomalous magnetic moment as a function of the absolute value of $y^{e\tau}y^{\tau e}$.

(Δa_e^H and $\Delta a_e^{h'}$), respectively, while the green solid line refers to their sum ($\Delta a_e^H + \Delta a_e^{h'}$). In addition, the horizontal yellow band indicates the 2.4σ discrepancy between the experimental measurement and theoretical prediction: $\Delta a_e = (-8.7 \pm 3.6) \times 10^{-13}$ [18]. We see that both h' and H have approximately the same positive contribution ($\simeq 10^{-13}$) to the total electron anomalous magnetic moment Δa_e at $|y^{e\tau}y^{\tau e}| = 0$, which is coming from e inside the loop (electron contribution). Additionally, since the contribution of τ inside the loop (tau contribution) which owes its sign to the product $y_{\tau e}^\phi y_{e\tau}^\phi$ is negative, Δa_e gets a negative contribution overall. This originates mainly from the H contribution (Δa_e^H), as it is clearly seen from Fig. 5. In this figure, the other relevant parameters have the benchmark values shown in Table I. It is clear that for $|y^{e\tau}y^{\tau e}| \simeq 5.6 \times 10^{-7}$, our benchmark sits near the central value for Δa_e ($= -8.7 \times 10^{-13}$).

V. DISCUSSION ON CONSTRAINTS

This section is devoted to a discussion of constraints that the proposed scenario must satisfy, and related issues as well as future tests of the various elements of our proposal. Subsection A focuses on bounds related to the additional $U(1)$ and its gauge boson and couplings, while Subsection B discusses constraints related to the scalar sector extension. We have, for the most part, restricted our discussion to the regions of parameter space relevant to our scenario.

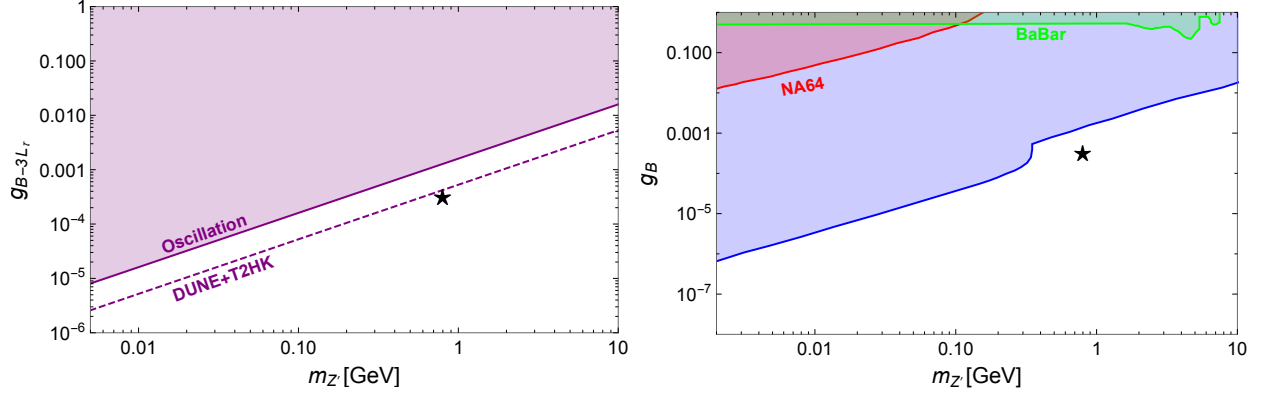


FIG. 6: Constraints on $m_{Z'}$ and g_{B-3L_τ} from oscillation experiments, denoted by the solid line and shaded region above it, along with projected sensitivities of T2K and DUNE (left panel, adapted from [144]) and on $m_{Z'}$ and g_B from NA64 [196] and BaBar [197], along with theoretical bounds from (see text) [198, 199] (right panel, adapted from [141]) along with our benchmark in Table I denoted by the black star.

A. The $U(1)$ extension

Constraints on $m_{Z'}$ and g_{B-3L_τ} : Strong constraints on this coupling and the associated Z' mass arise from oscillation experiments as well as various decay searches [137, 144, 164, 200]. Fig. 6 (left panel) shows these bounds, along with our benchmark point. We note that there is a significant difference between the bounds on the coupling coming from [144] and [137]. The reason lies in the choice, respectively, of the LMA and LMA + LMA-D and KamLAND solutions made by them. For more details the reader is referred to [201]. Our benchmark point is compatible with both bounds, comfortably with [144], but only marginally so with [137]. Future tests of these parameter values would be possible via oscillation measurements at DUNE [202] and T2HK [203], as discussed in [144]. Other experiments sensitive to τ interactions, like DONuT [204] and the future emulsion detectors SHiP [205], FASER ν [206, 207] and SND@LHC [208] could provide additional constraints on the parameter space for $m_{Z'}$ and g_{B-3L_τ} [209].

Constraints on $m_{Z'}$ and g_B : The gauging of baryon number via a light boson associated with a $U(1)_B$ symmetry, which primarily interacts with quarks is subject to a number of constraints on its mass $m_{Z'}$ and the gauge coupling g_B [141]. Assuming that the primary modes of decay are invisible, the strongest of these come from theoretically computed bounds arising from anomaly cancellation by heavy fermions, which lead to enhanced interaction

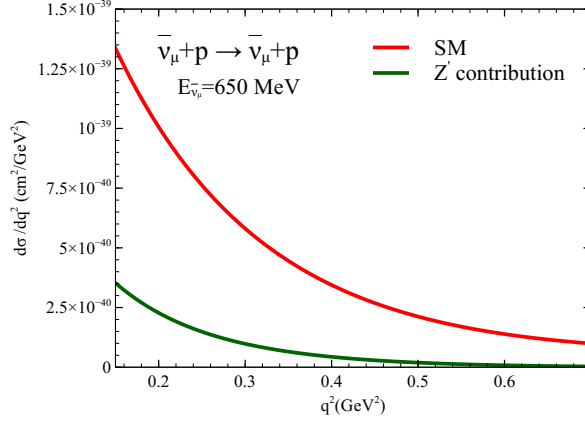


FIG. 7: The SM NC quasi-elastic anti-neutrino-proton cross section, compared to the contribution obtained from our model with the Z' due to its couplings to baryons and to ν_d . The parameter values used in calculating the Z' contributions are the same as those used for our MB result, and are given in Table I.

rates for processes involving the longitudinal mode of the Z' [198, 199]. In addition, constraints from searches by NA64 [196] and BaBar [197] for a light vector decaying to invisible become relevant. We show these in Fig. 6 (right panel), along with our benchmark values.

Contributions to NC ν -nucleon scattering at both low and high energies: At low energies, an important constraint arises from NC quasi-elastic neutrino-nucleon scattering, to which the new Z' would contribute via an amplitude proportional to $g_d g_B U_{\mu 4}$. MB has measured this cross section in the relevant range [108]. Fig. 7 shows the SM differential cross section for muon anti-neutrino scattering and compares it to the cross section from our model. We see that the contribution from the latter stays safely below the SM anti-neutrino cross section, which, of course, is lower than that for neutrinos and thus provides a more conservative basis for comparison. We note that our process with the Z' mediator does not distinguish between neutrino and anti-neutrino scattering, unlike the SM case. It also adds 10–25% to the SM cross section, over the range shown. Interestingly, MB NC measurements have been fitted with an axial mass M_A which is significantly higher than the value from the global average value of this parameter, indicating that the measured cross section is higher than expected, with one possible conclusion being that it is receiving contributions from new physics.

IceCube and DeepCore are a possible laboratory for new particles which are produced

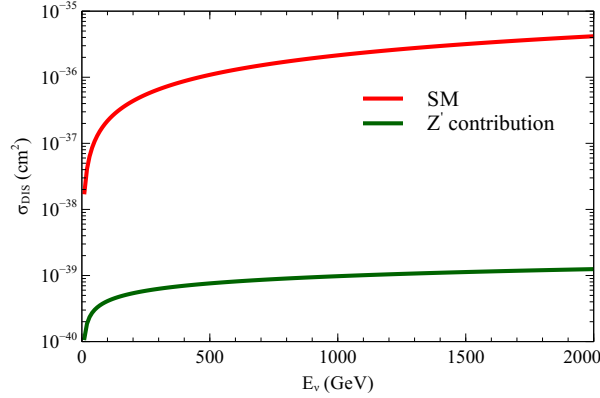


FIG. 8: The SM NC DIS cross section, compared to that obtained from our model. The parameter values used in calculating the Z' contribution are given in Table I.

via neutrino nucleon scattering [210, 211]. Fig. 8 shows our check for contributions of the model to deep inelastic scattering (DIS), comparing it to the SM total NC cross section for ν_μ -nucleon scattering. The Z' contributions are more than three orders of magnitude lower. We note that the DeepCore and IceCube detectors would be sensitive to the new particles and the interaction in our model in two ways: *a*) by a possibly measurable increase in the neutrino nucleon NC event rate, and *b*) via the decay of h' into an e^+e^- pair if, after its production in a NC event mediated by Z' , it travels a distance long enough to signal a double bang event (about 10 m in DeepCore, and \sim a few hundred m in IceCube). The lifetime of the h' in our scenario is $c\tau \sim 10^{-4}$ m. The distances travelled even at very high energies are much smaller than the resolution necessary to signal a double bang event. In addition, as Fig. 8 shows, the high energy NC cross section stays several orders of magnitude below the SM cross section. We note that similar to the low-energy case above, the Z' contribution has been calculated taking into account the enhancement it receives due to $g_d U_{\mu 4}$ at the neutrino vertex.

Constraints on $m_{\nu 4}$, $|U_{\mu 4}|$ and $|U_{e 4}|$: The mass of the dark neutrino in our model has a wider possible range than that in scenarios where it is required to decay inside the MB detector [78, 92, 93] to obtain the electron-like signal. Its main role here is that of a portal connecting the SM neutrinos via mixing to the Z' . Nonetheless, heavy sterile neutrino masses and mixings are tightly constrained by a number of experiments, as well as astrophysics and cosmology, and these bounds are discussed and summarized in [80–87, 212]. We assume that the ν_d does not constitute an appreciable fraction of DM in the universe, and has dominantly

invisible decay modes. Our benchmark value for its mass is ~ 50 MeV, and this along with the mixings we assume are in conformity with the existing bounds.

Constraints from NOMAD: The NOMAD experiment carried out a search for neutrino induced single photon events at high energies, $E_\nu \sim 25$ GeV [213]. It obtained an upper limit of 4.0×10^{-4} single photon events for every ν_μ induced charged-current event. Clearly, extrapolating our calculations to NOMAD energies would be invalid, given that the calculational procedures we use to obtain the pair production contributions do not apply there. NOMAD used coherent pion kinematics with one photon to arrive at their bound. We then examine the ratio of the cross section for our process, including coherent effects, to the charged current total inclusive incoherent muon production cross section measured by NOMAD at $E_\nu \sim 25$ GeV, and obtain a ratio below the upper bound given by NOMAD.

Constraints from CHARM II and MINERVA: We find that in our model, the Z' does contribute to the neutrino electron scattering cross section at these detectors to the extent of about $\sim 14\%$, leading to a very mild tension with their observations when flux and other uncertainties are accounted for.

Constraints from CE ν NS: Any additional $U(1)$ with a vector Z' mediator that couples to neutrinos and baryons could conceivably receive large contributions from coherent elastic neutrino-nucleon scattering (CE ν NS) [31, 32], since it would receive an enhancement proportional to the square of the number of nucleons. In our scenario, in spite of the choice of gauge groups being $U(1)_{B-3L\tau}$ or $U(1)_B$, the Z' does effectively couple to muon neutrinos (Fig. 1). The amplitude for this process receives an added enhancement from the fact that the effective active neutrino- Z' coupling is $g_d U_{\mu 4}$, which can be significantly larger than g_B .

The COHERENT Collaboration [214] has recently observed CE ν NS, for neutrinos in the energy range of $16 - 53$ MeV, and concurrently set stringent bounds on the parameters g_B and $m_{Z'}$. The values of g_B and $m_{Z'}$ chosen by us respect these constraints, but the coupling for the amplitude of the enhanced process, $g_B g_d U_{\mu 4}$ does not. However, the neutrino beam energies in COHERENT are below the kinematic range required for the process in Fig. 1, since besides nuclear/nucleon recoil, a heavy neutrino of mass ~ 50 MeV must be produced in the final state. Thus the event rate in COHERENT remains unaffected by our scenario.

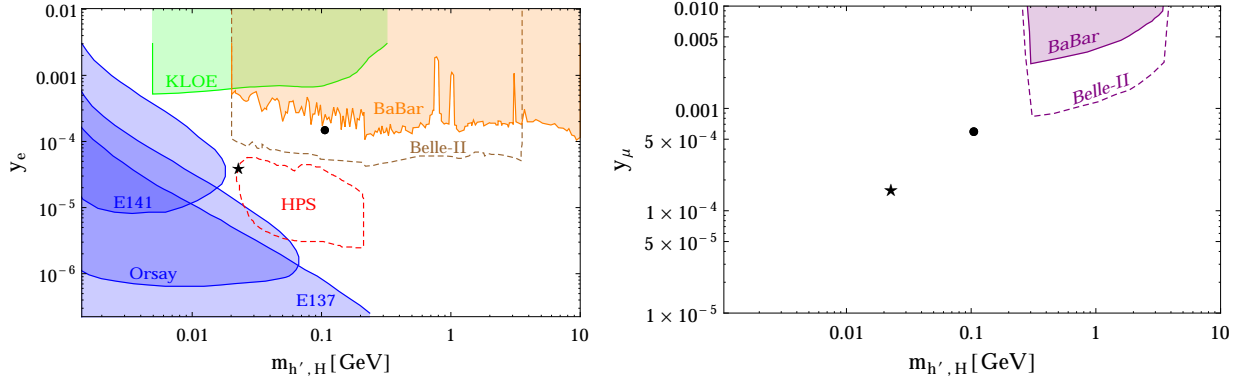


FIG. 9: Relevant constraints to our scenario, where the color shaded regions with solid boundary indicate to the excluded regions by current experiments, and the unshaded regions with dashed boundaries are future projections (see text for details).

B. The extended scalar sector

Constraints on y_e and $m_{h'}$ from dark photon searches: A dark photon search looks for its decay to lepton pair. These bounds can be translated [215, 216] to constraints on a light scalar which couples to leptons. We show these translated constraints relevant to our scenario from KLOE [217], BaBar [192] and the projected future sensitivity from Belle-II in Fig. 9 (left panel) [193].

Constraints on y_e and $m_{h'}$ from electron beam dump experiments: A light scalar with couplings to electrons could be searched for [125, 126] in beam dump experiments via its decay to an e^+e^- pair or photons. Relevant to the mass range under consideration here are the experiments E137 [218], E141 [219] and ORSAY [220]. The forbidden regions are shown in Fig. 9 (left panel). In the future, the HPS fixed target experiment [221] which will scatter electrons on tungsten, will be able to constrain the displaced decays of a light scalar. Its projected sensitivity is also shown in this figure.

Constraints from ND280: As discussed in [113], the T2K near-detector, ND280, is in a position to provide bounds on new physics related to the MB LEE. Relevant to our work here, the specific decay $h' \rightarrow e^+e^-$ could be observable in the Ar TPC associated with this detector. In our model, however, this decay is prompt, hence the Ar gas must act as both target and detection medium if this is to be observed. Since the target mass is only 16 kg, however, the number of events is unobservably small in our case.

Future tests of the muon and the electron $g - 2$: The E989 experiment [222] at Fermilab is soon likely to announce results of measurements of the muon $g - 2$ which will have significantly higher precision than current measurements. This will be complemented by measurements of this quantity at comparable precision by an experiment at J-PARC and the E34 Collaboration [223]. An important supplementary effort will be the measurement of the hadronic contributions to the muon magnetic moment by the MUonE experiment [224] at CERN, which will determine them at uncertainties below those in present theoretical calculations. Finally, continuing and improved measurements of the fine structure constant are likely to determine the future significance of the discrepancy in the electron $g - 2$.

Constraints on y_μ and m_H from colliders: BaBar has provided constraints [126, 193] on these parameters via their search for $e^+e^- \rightarrow \mu^+\mu^-\phi$, where ϕ is a generic light scalar. Also shown in Fig. 9 (right panel) is the future projection for Belle-II [193]. Our benchmark points, as shown, are below these bounds.

Constraints on y_τ and m_H from BaBar: Very recently, BaBar has provided strong constraints [225] on the parameter ξ , which is the ratio of the effective coupling ($y_{e,\mu,\tau}$ in our model) of a light scalar to a fermion compared to its SM Yukawa coupling (m_f/v). BaBar looks for narrow width decays of a leptophilic scalar ϕ , produced radiatively from τ -lepton via $e^+e^- \rightarrow \tau^+\tau^-\phi$, followed by $\phi \rightarrow e^+e^-$. In our case, noting that $y_{e,\mu,\tau}$ are all independent, this translates to a bound on y_τ and m_H . For our mass range for H , of 100 – 150 MeV, this implies that y_τ remain below $\approx 3.5 \times 10^{-3}$. In our scenario, y_τ , is independent and essentially free, and can be kept small. We also note that the independence of y_μ from y_τ in our scenario ensures that the bound on y_τ from BaBar does not automatically translate into a bound on y_μ , unlike the case where ξ is the same for all leptonic generations.

Constraints from $\tau \rightarrow e\gamma$: In our calculation for Δa_e , the $\text{BR}(\tau \rightarrow e\gamma)$ has a non-zero value due to the non-vanishing Yukawa couplings of the ϕ - e - τ interactions, $y_{\tau e(e\tau)}^\phi$. We thus calculated this $\text{BR}(\tau \rightarrow e\gamma)$ [226] mediated by the light scalars h' and H using $|y^{e\tau}y^{\tau e}| \simeq 5.6 \times 10^{-7}$. We find that this yields a total $\text{BR}(\tau \rightarrow e\gamma) \simeq 5.4 \times 10^{-10}$. We note that this is very small compared with the experimental upper bound, $\text{BR}(\tau \rightarrow e\gamma) < 1.1 \times 10^{-7}$ [195], and hence is not a concern.

Constraints from Higgs physics:. We note that in the model considered here, the h is almost identical to the SM Higgs, with negligible mixings to the other neutral scalars (h' and H). This makes the constraints from Higgs observations not a matter of immediate concern.

Stability of the scalar potential: We have examined the behaviour of the potential as the fields tend to infinity, in order to ensure it is stable. Our benchmark parameters satisfy the vacuum stability conditions. The details are provided in the Appendix B.

Collider constraints on the heavy charged CP-even scalars H^\pm : Drell-Yan processes at both LEP and the LHC can produce pairs of the H^\pm , which can subsequently decay to a neutrino and a lepton each. Bounds set on supersymmetric particles [227–229] which would mimic these final states can be translated to bounds on H^\pm , as discussed in [131, 230]. These lead to a lower bound on the charged scalar mass of $m_{H^\pm} > 110$ GeV.

Electro-weak precision constraints on the heavy charged CP-even scalars H^\pm and pseudoscalar A : The oblique parameters S, T and U are a measure of the effects new particles can have on gauge boson self energies. The effects of scalars in an expanded Higgs sector on these parameters have been discussed in [231–233]. For models in the alignment limit, bounds using the T parameter are particularly significant in constraining the plane of mass differences between a) the SM-like Higgs and the charged H^\pm , and b) the H^\pm and the pseudoscalar [131, 177]. Essentially, one finds that either the masses of the pair in a) or that in b) need to be close to each other, while the other mass difference can be large, *e.g.* \sim a few hundred GeV. In our scenario, if the dominant contribution to Δa_μ is to originate from an H with a mass below 200 MeV, one is led to the mass hierarchy $m_A \sim m_{H^\pm} \gg m_H$.

VI. SUMMARY AND CONCLUDING REMARKS

Among several anomalous signals at low energy experiments, the MB LEE and the discrepancy in the measured value of the anomalous magnetic moment of the muon stand out, due to their statistical significance, the duration over which they have been present and the scrutiny and interest they have generated. Our effort in this paper takes the viewpoint that these anomalies are due to interlinked underlying new physics involving a new $U(1)$ connecting the SM and the dark sector.

Pursuant to this, starting with the MB LEE, we find that a light Z' vector portal associated with $U(1)_{B-3L_\tau}$, which is anomaly-free, or a $U(1)_B$ extension of the SM, combined with a second Higgs doublet allows a very good fit to the excess. The Z' obtains its mass from a dark sector singlet scalar, and is coupled to a dark neutrino. The Higgs sector thus comprises of three CP-even scalars, h , which is predominantly SM Higgs-like, and h' and

H which are light compared to h and the charged Higgses of the model. h', H are coupled both to the dark sector and to SM fermions via mixing. In MB, the $h'(H)$ is produced via the $Z'-h'(H)-Z'$ coupling and decays primarily to an e^+e^- pair. Both h' and H contribute to both the MB LEE and the muon and electron $g-2$, but for our choice of benchmarks, the $h'(H)$ contributes dominantly to the MB LEE (the muon and electron $g-2$).

Our work underscores the role light scalars may play in understanding low energy anomalies that persist and survive further tests, and the possibility that a light Z' may provide an important portal to the dark sector. This Z' need not be unique as long as it couples in a flavor universal way to quarks. The couplings to leptons are constrained to be very small, however, especially for the first two generations. Overall, we provide a template for a model with an additional $U(1)$ that agrees very well with MB data while staying in conformity with all known constraints.

We note that a singlet scalar mass-mixed with the SM Higgs along with the Z' , could, in principle have provided an economical solution for the MB LEE. However, the fermionic couplings of such a scalar are constrained to be very tiny and cannot be used to generate the MB excess. This motivates the need for a second Higgs doublet mixed with the dark sector. We find that when incorporated, the interplay of the scalars via mixing allows us to understand both the MB signal and the observed anomalous value of the muon magnetic moment in a manner that satisfies existing constraints.

ACKNOWLEDGEMENTS

We are thankful to Richard Hill for discussions and collaboration in the early stages of this work. We thank William Louis and Tyler Thornton for help with the making of Fig. 2. RG would like to extend special thanks to Boris Kayser, William Louis and Geralyn Zeller for many very helpful discussions on MB and LSND results, and to Steven Dytman, Gerald Garvey, Sudip Jana and Lukas Koch for providing especially helpful clarifications over email. He is also grateful to Gauhar Abbas, Ismail Ahmed, N. Ananthanarayan, K. S. Babu, André de Gouvea, Jeff Dror, Rikard Enberg, Chris Hearty, Robert Lasenby, John LoSecco, Pedro Machado, Tanumoy Mondal, Biswarup Mukhopadhyaya, Satya Mukhopadhyay, Roberto Petti, Santosh Rai, S Uma Sankar and Ashoke Sen for helpful discussions and email communications. He thanks Patrick deNiverville, Suprabh Prakash and Sandeep

Sehrawat for assistance in the early stages of this work. He is grateful to the Theory Division and the Neutrino Physics Center at Fermilab for hospitality and visits where this work benefitted from discussions and a conducive environment. SR thanks KM Patel for useful discussions. He is grateful to Fermilab, where this work was initiated, for support via the Rajendran Raja Fellowship. WA, RG and SR also acknowledge support from the XII Plan Neutrino Project of the Department of Atomic Energy and the High Performance Cluster Facility at HRI (<http://www.hri.res.in/cluster/>).

APPENDICES

Appendix A: Diagonalization of CP-even Higgs mass matrix

In the basis (H_1^0, H_2^0, H_3^0) , the mass matrix of the neutral CP-even Higgses is given by

$$m_{\mathcal{H}}^2 = \begin{pmatrix} \lambda_1 v^2 & \lambda_6 v^2 & \lambda'_3 v v' \\ \lambda_6 v^2 & \bar{m}_H^2 & \lambda'_5 v v' \\ \lambda'_3 v v' & \lambda'_5 v v' & 2\lambda'_2 v'^2 \end{pmatrix}. \quad (\text{A1})$$

Now if $\lambda_6 \simeq 0 \simeq \lambda'_3$, then we get the alignment limit *i.e.* one of the CP-even Higgs mass eigenstates aligns with the vev direction of the scalar field. In the alignment limit, the mass matrix becomes

$$m_{\mathcal{H}}^2 \simeq \begin{pmatrix} \lambda_1 v^2 & 0 & 0 \\ 0 & \bar{m}_H^2 & \lambda'_5 v v' \\ 0 & \lambda'_5 v v' & 2\lambda'_2 v'^2 \end{pmatrix}. \quad (\text{A2})$$

Now,

$$Z^{\mathcal{H}} m_{\mathcal{H}}^2 (Z^{\mathcal{H}})^T = (\mathcal{M}^2)^{\text{diag}} = \text{diag}\{m_h^2, m_H^2, m_{h'}^2\}, \quad (\text{A3})$$

where

$$Z^{\mathcal{H}} = \begin{pmatrix} 1 & 0 & 0 \\ 0 & \cos \delta & -\sin \delta \\ 0 & \sin \delta & \cos \delta \end{pmatrix}, \quad \text{with} \quad \tan 2\delta = \frac{-2\lambda'_5 v v'}{\bar{m}_H^2 - 2\lambda'_2 v'^2}. \quad (\text{A4})$$

The eigenvalues of the mass matrix are

$$m_{h,H,h'}^2 \simeq \left\{ \lambda_1 v^2, \frac{1}{2} \left(\bar{m}_H^2 + 2\lambda'_2 v'^2 \pm \sqrt{(\bar{m}_H^2 - 2\lambda'_2 v'^2)^2 + 4(\lambda'_5 v v')^2} \right) \right\}. \quad (\text{A5})$$

If we choose $\bar{m}_H^2 = (102 \text{ MeV})^2$, $\lambda'_5 v v' = -(53.8 \text{ MeV})^2$ and $2\lambda'_2 v'^2 = (37 \text{ MeV})^2$, we get $m_H = 106 \text{ MeV}$, $m_{h'} = 23 \text{ MeV}$ and $\sin \delta = 0.28$, which fit our benchmark in Table I.

Appendix B: Vacuum Stability

For a stable vacuum, the potential should be bounded from below as the field strength approaches to infinity from any directions. In this limit, only the quartic part of the potential is relevant. In the alignment limit ($\lambda_6 \simeq 0 \simeq \lambda'_3$) and for simplicity we consider $\lambda_7 = 0 = \lambda'_4$. With those considerations, the quartic part of the potential becomes

$$V_4 = \frac{\lambda_1}{2}(\phi_h^\dagger \phi_h)(\phi_h^\dagger \phi_h) + \frac{\lambda_2}{2}(\phi_H^\dagger \phi_H)(\phi_H^\dagger \phi_H) + \lambda_3(\phi_h^\dagger \phi_h)(\phi_H^\dagger \phi_H) + \lambda_4(\phi_h^\dagger \phi_H)(\phi_H^\dagger \phi_h) + \frac{\lambda_5}{2}((\phi_h^\dagger \phi_H)^2 + (\phi_H^\dagger \phi_h)^2) + \lambda'_2(\phi_{h'}^* \phi_{h'})^2 + \lambda'_5(\phi_{h'}^* \phi_{h'}) (\phi_h^\dagger \phi_H + \phi_H^\dagger \phi_h). \quad (\text{B1})$$

We can parameterize the fields as [234]

$$|\phi_h| = r c_\vartheta s_\varphi, \quad |\phi_H| = r s_\vartheta s_\varphi, \quad |\phi_{h'}| = r c_\varphi, \quad \phi_h^\dagger \phi_H = |\phi_h| |\phi_H| \rho e^{i\gamma}, \quad (\text{B2})$$

where $s_x \equiv \sin x$, $c_x \equiv \cos x$, $r \geq 0$, $\vartheta \in [0, \pi/2]$, $\varphi \in [0, \pi/2]$, $\rho \in [0, 1]$ and $\gamma \in [0, 2\pi]$.

The potential can be written as

$$\frac{V_4}{r^4} = \left[\frac{\lambda_1}{2} c_\vartheta^4 + \frac{\lambda_2}{2} s_\vartheta^4 + \lambda_3 s_\vartheta^2 c_\vartheta^2 + \lambda_4 s_\vartheta^2 c_\vartheta^2 \rho^2 + \lambda_5 s_\vartheta^2 c_\vartheta^2 \rho^2 c_{2\gamma} \right] s_\varphi^4 + \lambda'_2 c_\varphi^4 + 2 \lambda'_5 \rho c_\vartheta s_\vartheta c^2 \phi s_\varphi^2 c_\gamma. \quad (\text{B3})$$

In our case, λ_4 is negative and other terms containing ρ are function of phase γ . Hence, we consider $\rho = 1$. Now,

$$(\lambda_5 s_\vartheta^2 c_\vartheta^2 c_{2\gamma} s_\varphi^4 + 2 \lambda'_5 c_\vartheta s_\vartheta c_\varphi^2 s_\varphi^2 c_\gamma)_{\min} > (-|\lambda_5| s_\vartheta^2 c_\vartheta^2 s_\varphi^4 - 2|\lambda'_5| c_\vartheta s_\vartheta c_\varphi^2 s_\varphi^2). \quad (\text{B4})$$

We define

$$\frac{\tilde{V}_4}{r^4} = \left[\frac{\lambda_1}{2} c_\vartheta^4 + \frac{\lambda_2}{2} s_\vartheta^4 + \lambda_3 s_\vartheta^2 c_\vartheta^2 + \lambda_4 s_\vartheta^2 c_\vartheta^2 - |\lambda_5| s_\vartheta^2 c_\vartheta^2 \right] s_\varphi^4 + \lambda'_2 c_\varphi^4 - 2|\lambda'_5| c_\vartheta s_\vartheta c_\varphi^2 s_\varphi^2. \quad (\text{B5})$$

Now, $\tilde{V}_4 > 0$ implies that $V_4 > 0$. We first calculate the values of \tilde{V}_4/r^4 at the boundary points in the (ϑ, φ) plane:

$$\begin{aligned} \frac{\tilde{V}_4}{r^4} \left(\vartheta = 0, \varphi = \frac{\pi}{2} \right) &= \frac{\lambda_1}{2} > 0, \quad \frac{\tilde{V}_4}{r^4} \left(\vartheta = \frac{\pi}{2}, \varphi = \frac{\pi}{2} \right) = \frac{\lambda_2}{2} > 0, \quad \frac{\tilde{V}_4}{r^4} (\varphi = 0) = \lambda'_2 > 0, \\ \frac{\tilde{V}_4}{r^4} \left(\varphi = \frac{\pi}{2} \right) &= \frac{\lambda_1}{2} c_\vartheta^4 + \frac{\lambda_2}{2} s_\vartheta^4 + (\lambda_3 + \lambda_4 - |\lambda_5|) s_\vartheta^2 c_\vartheta^2 > 0. \end{aligned}$$

Therefore, the vacuum stability conditions can be written as

$$\lambda_1, \lambda_2, \lambda'_2 > 0, \quad (\text{B6})$$

and

$$\lambda_3 + \lambda_4 - |\lambda_5| > -\sqrt{\lambda_1 \lambda_2}. \quad (\text{B7})$$

Also, we have to show that $\tilde{V}_4/r^4 > 0$ in the interior points (ϑ, φ) , *i.e.*

$$-2|\lambda'_5|c_\vartheta s_\vartheta > -\left[\frac{\lambda_1}{2}c_\vartheta^4 + \frac{\lambda_2}{2}s_\vartheta^4 + (\lambda_3 + \lambda_4 - |\lambda_5|)s_\vartheta^2 c_\vartheta^2\right]\tan^2 \varphi - \frac{\lambda'_2}{\tan^2 \varphi}. \quad (\text{B8})$$

Maximizing the right hand side of the inequality (B8) with respect to φ , we get

$$-|\lambda'_5|c_\vartheta s_\vartheta > -\sqrt{\lambda'_2 \left(\frac{\lambda_1}{2}c_\vartheta^4 + \frac{\lambda_2}{2}s_\vartheta^4 + (\lambda_3 + \lambda_4 - |\lambda_5|)s_\vartheta^2 c_\vartheta^2\right)}. \quad (\text{B9})$$

Thus, we get the final condition for a stable vacuum as

$$(\lambda_3 + \lambda_4 - |\lambda_5|)\lambda'_2 - |\lambda'_5|^2 > -\lambda'_2 \sqrt{\lambda_1 \lambda_2}. \quad (\text{B10})$$

-
- [1] M. Tanabashi et al. (Particle Data Group), Phys. Rev. **D98**, 030001 (2018).
 - [2] C. Quigg, *Gauge Theories of the Strong, Weak, and Electromagnetic Interactions: Second Edition* (Princeton University Press, USA, 2013).
 - [3] P. B. Pal, *An Introductory Course of Particle Physics* (CRC Press, 2014).
 - [4] K. Arun, S. B. Gudennavar, and C. Sivaram, Adv. Space Res. **60**, 166 (2017), 1704.06155.
 - [5] F. Kahlhoefer, Int. J. Mod. Phys. **A32**, 1730006 (2017), 1702.02430.
 - [6] J. M. Gaskins, Contemp. Phys. **57**, 496 (2016), 1604.00014.
 - [7] G. Bertone, D. Hooper, and J. Silk, Phys. Rept. **405**, 279 (2005), hep-ph/0404175.
 - [8] J. L. Feng, Ann. Rev. Astron. Astrophys. **48**, 495 (2010), 1003.0904.
 - [9] S. Pascoli and J. Turner, Nature **580**, 323 (2020).
 - [10] L. Canetti, M. Drewes, and M. Shaposhnikov, New J. Phys. **14**, 095012 (2012), 1204.4186.
 - [11] Q. R. Ahmad et al. (SNO), Phys. Rev. Lett. **87**, 071301 (2001), nucl-ex/0106015.
 - [12] Y. Fukuda et al. (Super-Kamiokande), Phys. Rev. Lett. **81**, 1562 (1998), hep-ex/9807003.
 - [13] K. Abe, N. Abgrall, H. Aihara, T. Akiri, J. B. Albert, C. Andreopoulos, S. Aoki, A. Ariga, T. Ariga, S. Assylbekov, et al. (T2K Collaboration), Phys. Rev. D **88**, 032002 (2013).
 - [14] J. K. Ahn et al. (RENO), Phys. Rev. Lett. **108**, 191802 (2012), 1204.0626.
 - [15] S. P. Martin, pp. 1–98 (1997), [Adv. Ser. Direct. High Energy Phys.18,1(1998)], hep-ph/9709356.

- [16] J. P. Miller, E. de Rafael, and B. Roberts, Rept. Prog. Phys. **70**, 795 (2007), hep-ph/0703049.
- [17] T. Aoyama et al., Phys. Rept. **887**, 1 (2020), 2006.04822.
- [18] R. H. Parker, C. Yu, W. Zhong, B. Estey, and H. Müller, Science **360**, 191 (2018), 1812.04130.
- [19] M. Maltoni (2018), URL <https://doi.org/10.5281/zenodo.1287015>.
- [20] J. Ahn et al. (KOTO), Phys. Rev. Lett. **122**, 021802 (2019), 1810.09655.
- [21] D. London, in *11th International Symposium on Quantum Theory and Symmetries* (2019), 1911.06238.
- [22] L. Delle Rose, S. Khalil, S. J. King, and S. Moretti, Front. in Phys. **7**, 73 (2019), 1812.05497.
- [23] M. Pospelov, Phys. Rev. **D84**, 085008 (2011), 1103.3261.
- [24] R. Harnik, J. Kopp, and P. A. N. Machado, JCAP **1207**, 026 (2012), 1202.6073.
- [25] M. Pospelov and J. Pradler, Phys. Rev. **D85**, 113016 (2012), [Erratum: Phys. Rev.D88,no.3,039904(2013)], 1203.0545.
- [26] B. Batell, M. Pospelov, and B. Shuve, JHEP **08**, 052 (2016), 1604.06099.
- [27] D. McKeen and N. Raj, Phys. Rev. **D99**, 103003 (2019), 1812.05102.
- [28] M. Blennow, E. Fernandez-Martinez, A. Olivares-Del Campo, S. Pascoli, S. Rosauero-Alcaraz, and A. V. Titov, Eur. Phys. J. **C79**, 555 (2019), 1903.00006.
- [29] P. Ballett, M. Hostert, and S. Pascoli (2019), 1903.07589.
- [30] C. A. Argüelles et al. (2019), 1907.08311.
- [31] D. Z. Freedman, Phys. Rev. D **9**, 1389 (1974).
- [32] V. B. Kopeliovich and L. L. Frankfurt, JETP Lett. **19**, 145 (1974), [Pisma Zh. Eksp. Teor. Fiz.19,236(1974)].
- [33] J. Billard, L. Strigari, and E. Figueroa-Feliciano, Phys. Rev. **D89**, 023524 (2014), 1307.5458.
- [34] P. deNiverville, M. Pospelov, and A. Ritz, Phys. Rev. **D84**, 075020 (2011), 1107.4580.
- [35] P. deNiverville, D. McKeen, and A. Ritz, Phys. Rev. **D86**, 035022 (2012), 1205.3499.
- [36] R. Dharmapalan et al. (MiniBooNE) (2012), 1211.2258.
- [37] B. Batell, P. deNiverville, D. McKeen, M. Pospelov, and A. Ritz, Phys. Rev. **D90**, 115014 (2014), 1405.7049.
- [38] P. deNiverville, M. Pospelov, and A. Ritz, Phys. Rev. **D92**, 095005 (2015), 1505.07805.
- [39] P. deNiverville, C.-Y. Chen, M. Pospelov, and A. Ritz, Phys. Rev. **D95**, 035006 (2017), 1609.01770.
- [40] A. A. Aguilar-Arevalo et al. (MiniBooNE), Phys. Rev. Lett. **118**, 221803 (2017), 1702.02688.

- [41] A. A. Aguilar-Arevalo et al. (MiniBooNE DM), Phys. Rev. **D98**, 112004 (2018), 1807.06137.
- [42] P. deNiverville and C. Frugiuele, Phys. Rev. **D99**, 051701 (2019), 1807.06501.
- [43] A. Bhattacharya, R. Gandhi, and A. Gupta, JCAP **1503**, 027 (2015), 1407.3280.
- [44] J. Kopp, J. Liu, and X.-P. Wang, JHEP **04**, 105 (2015), 1503.02669.
- [45] A. Bhattacharya, R. Gandhi, A. Gupta, and S. Mukhopadhyay, JCAP **1705**, 002 (2017), 1612.02834.
- [46] C. A. Argüelles and H. Dujmovic (IceCube), in *36th International Cosmic Ray Conference (ICRC 2019) Madison, Wisconsin, USA, July 24-August 1, 2019* (2019), 1907.11193.
- [47] M. W. Winkler, Phys. Rev. D **99**, 015018 (2019), 1809.01876.
- [48] A. A. Aguilar-Arevalo et al. (MiniBooNE), Phys. Rev. Lett. **98**, 231801 (2007), 0704.1500.
- [49] A. A. Aguilar-Arevalo et al. (MiniBooNE), Phys. Rev. Lett. **102**, 101802 (2009), 0812.2243.
- [50] A. A. Aguilar-Arevalo et al. (MiniBooNE), Phys. Rev. Lett. **105**, 181801 (2010), 1007.1150.
- [51] A. A. Aguilar-Arevalo et al. (MiniBooNE), Phys. Rev. Lett. **110**, 161801 (2013), 1303.2588.
- [52] A. A. Aguilar-Arevalo et al. (MiniBooNE), Phys. Rev. Lett. **121**, 221801 (2018), 1805.12028.
- [53] A. Aguilar-Arevalo et al. (MiniBooNE) (2020), 2006.16883.
- [54] A. Aguilar-Arevalo et al. (LSND), Phys. Rev. **D64**, 112007 (2001), hep-ex/0104049.
- [55] K. Eitel, Progress in Particle and Nuclear Physics **48**, 89 (2002), ISSN 0146-6410.
- [56] M. A. Acero, C. Giunti, and M. Laveder, Phys. Rev. **D78**, 073009 (2008), 0711.4222.
- [57] C. Giunti and M. Laveder, Phys. Rev. **C83**, 065504 (2011), 1006.3244.
- [58] T. A. Mueller et al., Phys. Rev. **C83**, 054615 (2011), 1101.2663.
- [59] G. Mention, M. Fechner, T. Lasserre, T. A. Mueller, D. Lhuillier, M. Cribier, and A. Letourneau, Phys. Rev. **D83**, 073006 (2011), 1101.2755.
- [60] P. Huber, Phys. Rev. **C84**, 024617 (2011), [Erratum: Phys. Rev.C85,029901(2012)], 1106.0687.
- [61] A. C. Hayes, J. L. Friar, G. T. Garvey, G. Jungman, and G. Jonkmans, Phys. Rev. Lett. **112**, 202501 (2014), 1309.4146.
- [62] A. C. Hayes and P. Vogel, Ann. Rev. Nucl. Part. Sci. **66**, 219 (2016), 1605.02047.
- [63] Y. J. Ko et al. (NEOS), Phys. Rev. Lett. **118**, 121802 (2017), 1610.05134.
- [64] I. Alekseev et al., JINST **11**, P11011 (2016), 1606.02896.
- [65] P. Adamson et al. (MINOS+), Phys. Rev. Lett. **122**, 091803 (2019), 1710.06488.
- [66] M. G. Aartsen et al. (IceCube), Phys. Rev. Lett. **117**, 071801 (2016), 1605.01990.

- [67] K. N. Abazajian et al. (2012), 1204.5379.
- [68] G. H. Collin, C. A. Argüelles, J. M. Conrad, and M. H. Shaevitz, Nucl. Phys. **B908**, 354 (2016), 1602.00671.
- [69] G. H. Collin, C. A. Argüelles, J. M. Conrad, and M. H. Shaevitz, Phys. Rev. Lett. **117**, 221801 (2016), 1607.00011.
- [70] J. M. Conrad and M. H. Shaevitz, Adv. Ser. Direct. High Energy Phys. **28**, 391 (2018), 1609.07803.
- [71] S. Gariazzo, C. Giunti, M. Laveder, and Y. F. Li, JHEP **06**, 135 (2017), 1703.00860.
- [72] M. Dentler, A. Hernández-Cabezudo, J. Kopp, P. A. Machado, M. Maltoni, I. Martinez-Soler, and T. Schwetz, JHEP **08**, 010 (2018), 1803.10661.
- [73] A. Diaz, C. A. Argüelles, G. H. Collin, J. M. Conrad, and M. H. Shaevitz (2019), 1906.00045.
- [74] R. H. Cyburt, B. D. Fields, K. A. Olive, and T.-H. Yeh, Rev. Mod. Phys. **88**, 015004 (2016), 1505.01076.
- [75] P. A. R. Ade et al. (Planck), Astron. Astrophys. **594**, A13 (2016), 1502.01589.
- [76] S. Palomares-Ruiz, S. Pascoli, and T. Schwetz, JHEP **09**, 048 (2005), hep-ph/0505216.
- [77] S. N. Gninenko, Phys. Rev. Lett. **103**, 241802 (2009), 0902.3802.
- [78] S. N. Gninenko, Phys. Rev. **D83**, 015015 (2011), 1009.5536.
- [79] M. Masip, P. Masjuan, and D. Meloni, JHEP **01**, 106 (2013), 1210.1519.
- [80] P. D. Bolton, F. F. Deppisch, and P. Bhupal Dev, JHEP **03**, 170 (2020), 1912.03058.
- [81] A. Atre, T. Han, S. Pascoli, and B. Zhang, JHEP **05**, 030 (2009), 0901.3589.
- [82] D. McKeen and M. Pospelov, Phys. Rev. **D82**, 113018 (2010), 1011.3046.
- [83] V. A. Duk et al. (ISTRA+), Phys. Lett. **B710**, 307 (2012), 1110.1610.
- [84] M. Drewes and B. Garbrecht, Nucl. Phys. **B921**, 250 (2017), 1502.00477.
- [85] A. de Gouvêa and A. Kobach, Phys. Rev. **D93**, 033005 (2016), 1511.00683.
- [86] D. A. Bryman and R. Shrock, Phys. Rev. **D100**, 053006 (2019), 1904.06787.
- [87] D. A. Bryman and R. Shrock (2019), 1909.11198.
- [88] Y. Bai, R. Lu, S. Lu, J. Salvado, and B. A. Stefanek, Phys. Rev. **D93**, 073004 (2016), 1512.05357.
- [89] J. Liao and D. Marfatia, Phys. Rev. Lett. **117**, 071802 (2016), 1602.08766.
- [90] M. Carena, Y.-Y. Li, C. S. Machado, P. A. N. Machado, and C. E. M. Wagner, Phys. Rev. **D96**, 095014 (2017), 1708.09548.

- [91] J. Asaadi, E. Church, R. Guenette, B. J. P. Jones, and A. M. Szelc, Phys. Rev. **D97**, 075021 (2018), 1712.08019.
- [92] E. Bertuzzo, S. Jana, P. A. N. Machado, and R. Zukanovich Funchal, Phys. Rev. Lett. **121**, 241801 (2018), 1807.09877.
- [93] P. Ballett, S. Pascoli, and M. Ross-Lonergan, Phys. Rev. **D99**, 071701 (2019), 1808.02915.
- [94] A. Ioannisian (2019), 1909.08571.
- [95] O. Fischer, A. Hernández-Cabezudo, and T. Schwetz, Phys. Rev. D **101**, 075045 (2020), 1909.09561.
- [96] M. Dentler, I. Esteban, J. Kopp, and P. Machado, Phys. Rev. D **101**, 115013 (2020), 1911.01427.
- [97] A. de Gouvêa, O. L. G. Peres, S. Prakash, and G. V. Stenico, JHEP **07**, 141 (2020), 1911.01447.
- [98] A. Datta, S. Kamali, and D. Marfatia, Phys. Lett. B **807**, 135579 (2020), 2005.08920.
- [99] B. Dutta, S. Ghosh, and T. Li, Phys. Rev. D **102**, 055017 (2020), 2006.01319.
- [100] A. Abdullahi, M. Hostert, and S. Pascoli (2020), 2007.11813.
- [101] L. B. Auerbach et al. (LSND), Phys. Rev. **D63**, 112001 (2001), hep-ex/0101039.
- [102] M. Deniz et al. (TEXONO), Phys. Rev. **D81**, 072001 (2010), 0911.1597.
- [103] G. Bellini et al., Phys. Rev. Lett. **107**, 141302 (2011), 1104.1816.
- [104] J. Park, Ph.D. thesis, University of Rochester (2013), URL <http://lss.fnal.gov/archive/thesis/2000/fermilab-thesis-2013-36.shtml>.
- [105] P. Vilain, G. Wilquet, R. Beyer, W. Flegel, H. Grote, T. Mouthuy, H. Øveras, J. Panman, A. Rozanov, K. Winter, et al., Physics Letters B **335**, 246 (1994), ISSN 0370-2693.
- [106] S. Bilmis, I. Turan, T. M. Aliev, M. Deniz, L. Singh, and H. T. Wong, Phys. Rev. **D92**, 033009 (2015), 1502.07763.
- [107] C. A. Argüelles, M. Hostert, and Y.-D. Tsai, Phys. Rev. Lett. **123**, 261801 (2019), 1812.08768.
- [108] D. Perevalov and R. Tayloe (MiniBooNE), AIP Conf. Proc. **1189**, 175 (2009), 0909.4617.
- [109] R. Gandhi, C. Quigg, M. H. Reno, and I. Sarcevic, Astropart. Phys. **5**, 81 (1996), hep-ph/9512364.
- [110] R. Gandhi, C. Quigg, M. H. Reno, and I. Sarcevic, Phys. Rev. **D58**, 093009 (1998), hep-ph/9807264.
- [111] A. Cooper-Sarkar, P. Mertsch, and S. Sarkar, JHEP **08**, 042 (2011), 1106.3723.

- [112] S. Chekanov et al. (ZEUS), Phys. Rev. **D67**, 012007 (2003), hep-ex/0208023.
- [113] V. Brdar, O. Fischer, and A. Y. Smirnov (2020), 2007.14411.
- [114] G. Bennett et al. (Muon g-2), Phys. Rev. D **73**, 072003 (2006), hep-ex/0602035.
- [115] H. Brown et al. (Muon g-2), Phys. Rev. Lett. **86**, 2227 (2001), hep-ex/0102017.
- [116] F. Jegerlehner and A. Nyffeler, Phys. Rept. **477**, 1 (2009), 0902.3360.
- [117] M. Lindner, M. Platscher, and F. S. Queiroz, Phys. Rept. **731**, 1 (2018), 1610.06587.
- [118] J. L. Holzbauer, J. Phys. Conf. Ser. **770**, 012038 (2016), 1610.10069.
- [119] M. Davier, A. Hoecker, B. Malaescu, and Z. Zhang, Eur. Phys. J. C **80**, 241 (2020), [Erratum: Eur.Phys.J.C 80, 410 (2020)], 1908.00921.
- [120] T. Kinoshita and W. J. Marciano, *Theory of the muon anomalous magnetic moment* (1990), vol. 7, pp. 419–478.
- [121] Y.-F. Zhou and Y.-L. Wu, Eur. Phys. J. C **27**, 577 (2003), hep-ph/0110302.
- [122] V. Barger, C.-W. Chiang, W.-Y. Keung, and D. Marfatia, Phys. Rev. Lett. **106**, 153001 (2011), 1011.3519.
- [123] D. Tucker-Smith and I. Yavin, Phys. Rev. D **83**, 101702 (2011), 1011.4922.
- [124] C.-Y. Chen, H. Davoudiasl, W. J. Marciano, and C. Zhang, Phys. Rev. D **93**, 035006 (2016), 1511.04715.
- [125] Y.-S. Liu, D. McKeen, and G. A. Miller, Phys. Rev. Lett. **117**, 101801 (2016), 1605.04612.
- [126] B. Batell, N. Lange, D. McKeen, M. Pospelov, and A. Ritz, Phys. Rev. D **95**, 075003 (2017), 1606.04943.
- [127] W. Marciano, A. Masiero, P. Paradisi, and M. Passera, Phys. Rev. D **94**, 115033 (2016), 1607.01022.
- [128] L. Wang, J. M. Yang, and Y. Zhang, Nucl. Phys. B **924**, 47 (2017), 1610.05681.
- [129] J. Liu, C. E. Wagner, and X.-P. Wang, JHEP **03**, 008 (2019), 1810.11028.
- [130] J. Liu, N. McGinnis, C. E. Wagner, and X.-P. Wang, JHEP **04**, 197 (2020), 2001.06522.
- [131] S. Jana, V. P. K., and S. Saad, Phys. Rev. D **101**, 115037 (2020), 2003.03386.
- [132] B. C. Allanach, J. Davighi, and S. Melville, JHEP **02**, 082 (2019), [erratum: JHEP08,064(2019)], 1812.04602.
- [133] R. Foot, Mod. Phys. Lett. **A6**, 527 (1991).
- [134] X. G. He, G. C. Joshi, H. Lew, and R. R. Volkas, Phys. Rev. D **43**, R22 (1991).
- [135] X.-G. He, G. C. Joshi, H. Lew, and R. R. Volkas, Phys. Rev. D **44**, 2118 (1991).

- [136] T. Araki, J. Heeck, and J. Kubo, JHEP **07**, 083 (2012), 1203.4951.
- [137] J. Heeck, M. Lindner, W. Rodejohann, and S. Vogl, SciPost Phys. **6**, 038 (2019), 1812.04067.
- [138] J. Kopp, J. Phys. Conf. Ser. **485**, 012032 (2014), 1210.2703.
- [139] J. Heeck, Phys. Lett. **B739**, 256 (2014), 1408.6845.
- [140] Y. S. Jeong, C. S. Kim, and H.-S. Lee, Int. J. Mod. Phys. **A31**, 1650059 (2016), 1512.03179.
- [141] P. Ilten, Y. Soreq, M. Williams, and W. Xue, JHEP **06**, 004 (2018), 1801.04847.
- [142] M. Bauer, P. Foldenauer, and J. Jaeckel, JHEP **07**, 094 (2018), [JHEP18,094(2020)], 1803.05466.
- [143] M. Abdullah, J. B. Dent, B. Dutta, G. L. Kane, S. Liao, and L. E. Strigari, Phys. Rev. **D98**, 015005 (2018), 1803.01224.
- [144] T. Han, J. Liao, H. Liu, and D. Marfatia, JHEP **11**, 028 (2019), 1910.03272.
- [145] E. Ma, Phys. Lett. B **433**, 74 (1998), hep-ph/9709474.
- [146] E. Ma and D. Roy, Phys. Rev. D **58**, 095005 (1998), hep-ph/9806210.
- [147] E. Ma and U. Sarkar, Phys. Lett. B **439**, 95 (1998), hep-ph/9807307.
- [148] A. E. Nelson and N. Tetradis, Physics Letters B **221**, 80 (1989), ISSN 0370-2693.
- [149] J. Collins, F. Wilczek, and A. Zee, Phys. Rev. D **18**, 242 (1978).
- [150] X.-G. He and S. Rajpoot, Phys. Rev. **D41**, 1636 (1990).
- [151] R. Foot, G. C. Joshi, and H. Lew, Phys. Rev. D **40**, 2487 (1989).
- [152] C. D. Carone and H. Murayama, Phys. Rev. Lett. **74**, 3122 (1995), hep-ph/9411256.
- [153] C. D. Carone and H. Murayama, Phys. Rev. D **52**, 484 (1995), hep-ph/9501220.
- [154] P. Fileviez Perez and M. B. Wise, Phys. Rev. **D82**, 011901 (2010), [Erratum: Phys. Rev.D82,079901(2010)], 1002.1754.
- [155] T. R. Dulaney, P. Fileviez Perez, and M. B. Wise, Phys. Rev. **D83**, 023520 (2011), 1005.0617.
- [156] P. V. Dong and H. N. Long (2010), [Phys. Int.6,23(2015)], 1010.3818.
- [157] P. Ko and Y. Omura, Phys. Lett. **B701**, 363 (2011), 1012.4679.
- [158] M. Buckley, P. Fileviez Perez, D. Hooper, and E. Neil, Phys. Lett. **B702**, 256 (2011), 1104.3145.
- [159] P. Fileviez Perez and M. B. Wise, Phys. Rev. **D84**, 055015 (2011), 1105.3190.
- [160] P. Fileviez Perez and M. B. Wise, JHEP **08**, 068 (2011), 1106.0343.
- [161] R. F. Lebed and V. E. Mayes, Phys. Rev. **D84**, 075016 (2011), 1106.4347.
- [162] M. L. Graesser, I. M. Shoemaker, and L. Vecchi (2011), 1107.2666.

- [163] B. A. Dobrescu and C. Frugiuele, Phys. Rev. Lett. **113**, 061801 (2014), 1404.3947.
- [164] S. Tulin, Phys. Rev. **D89**, 114008 (2014), 1404.4370.
- [165] P. Fileviez Pérez, E. Golias, R.-H. Li, and C. Murgui, Phys. Rev. **D99**, 035009 (2019), 1810.06646.
- [166] B. Holdom, Phys. Lett. **166B**, 196 (1986).
- [167] H. Davoudiasl, H.-S. Lee, and W. J. Marciano, Phys. Rev. **D85**, 115019 (2012), 1203.2947.
- [168] C. Cheung, J. T. Ruderman, L.-T. Wang, and I. Yavin, Phys. Rev. D **80**, 035008 (2009), 0902.3246.
- [169] R. Essig et al., in *Proceedings, 2013 Community Summer Study on the Future of U.S. Particle Physics: Snowmass on the Mississippi (CSS2013): Minneapolis, MN, USA, July 29-August 6, 2013* (2013), 1311.0029.
- [170] H. Davoudiasl, H.-S. Lee, and W. J. Marciano, Phys. Rev. Lett. **109**, 031802 (2012), 1205.2709.
- [171] T. Lee, Phys. Rev. D **8**, 1226 (1973).
- [172] G. Branco, P. Ferreira, L. Lavoura, M. Rebelo, M. Sher, and J. P. Silva, Phys. Rept. **516**, 1 (2012), 1106.0034.
- [173] O. Lebedev and Y. Mambrini, Phys. Lett. **B734**, 350 (2014), 1403.4837.
- [174] P. J. Fox, J. Liu, D. Tucker-Smith, and N. Weiner, Phys. Rev. D **84**, 115006 (2011), 1104.4127.
- [175] G. C. Branco, L. Lavoura, and J. P. Silva, *CP Violation*, vol. 103 (1999).
- [176] S. Davidson and H. E. Haber, Phys. Rev. D **72**, 035004 (2005), [Erratum: Phys.Rev.D 72, 099902 (2005)], hep-ph/0504050.
- [177] K. Babu and S. Jana, JHEP **02**, 193 (2019), 1812.11943.
- [178] R. J. Hill and G. Paz, Phys. Rev. D **82**, 113005 (2010), 1008.4619.
- [179] R. J. Hill, Phys. Rev. **D81**, 013008 (2010), 0905.0291.
- [180] J. R. Jordan, Y. Kahn, G. Krnjaic, M. Moschella, and J. Spitz, Phys. Rev. Lett. **122**, 081801 (2019), 1810.07185.
- [181] G. S. Karagiorgi, Ph.D. thesis, Massachusetts Institute of Technology (2010).
- [182] F. Staub (2008), 0806.0538.
- [183] F. Staub, Comput. Phys. Commun. **185**, 1773 (2014), 1309.7223.
- [184] J. Alwall, R. Frederix, S. Frixione, V. Hirschi, F. Maltoni, O. Mattelaer, H. S. Shao, T. Stelzer, P. Torrielli, and M. Zaro, JHEP **07**, 079 (2014), 1405.0301.

- [185] C. Athanassopoulos et al. (LSND), Phys. Rev. Lett. **75**, 2650 (1995), nucl-ex/9504002.
- [186] C. Athanassopoulos et al. (LSND), Phys. Rev. Lett. **77**, 3082 (1996), nucl-ex/9605003.
- [187] C. Athanassopoulos, L. B. Auerbach, R. L. Burman, I. Cohen, D. O. Caldwell, B. D. Dieterle, J. B. Donahue, A. M. Eisner, A. Fazely, F. J. Federspiel, et al., Phys. Rev. C **54**, 2685 (1996).
- [188] C. Athanassopoulos, L. B. Auerbach, R. L. Burman, D. O. Caldwell, E. D. Church, I. Cohen, J. B. Donahue, A. Fazely, F. J. Federspiel, G. T. Garvey, et al. (LSND Collaboration), Phys. Rev. C **58**, 2489 (1998).
- [189] M. Betancourt et al., Phys. Rept. **773-774**, 1 (2018), 1805.07378.
- [190] R. Jackiw and S. Weinberg, Phys. Rev. D **5**, 2396 (1972).
- [191] J. P. Leveille, Nucl. Phys. B **137**, 63 (1978).
- [192] J. Lees et al. (BaBar), Phys. Rev. Lett. **113**, 201801 (2014), 1406.2980.
- [193] B. Batell, A. Freitas, A. Ismail, and D. Mckeen, Phys. Rev. D **98**, 055026 (2018), 1712.10022.
- [194] A. Baldini et al. (MEG), Eur. Phys. J. C **76**, 434 (2016), 1605.05081.
- [195] B. Aubert et al. (BaBar), Phys. Rev. Lett. **104**, 021802 (2010), 0908.2381.
- [196] D. Banerjee et al. (NA64), Phys. Rev. D **97**, 072002 (2018), 1710.00971.
- [197] J. Lees et al. (BaBar), Phys. Rev. Lett. **119**, 131804 (2017), 1702.03327.
- [198] J. A. Dror, R. Lasenby, and M. Pospelov, Phys. Rev. Lett. **119**, 141803 (2017), 1705.06726.
- [199] J. A. Dror, R. Lasenby, and M. Pospelov, Phys. Rev. **D96**, 075036 (2017), 1707.01503.
- [200] Y. Farzan and J. Heeck, Phys. Rev. D **94**, 053010 (2016), 1607.07616.
- [201] I. Esteban, M. Gonzalez-Garcia, M. Maltoni, I. Martinez-Soler, and J. Salvado, JHEP **08**, 180 (2018), 1805.04530.
- [202] R. Acciarri et al. (DUNE) (2015), 1512.06148.
- [203] K. Abe et al. (Hyper-Kamiokande) (2018), 1805.04163.
- [204] K. Kodama et al. (DONuT), Phys. Rev. D **78**, 052002 (2008), 0711.0728.
- [205] M. Anelli et al. (SHiP) (2015), 1504.04956.
- [206] H. Abreu et al. (FASER) (2020), 2001.03073.
- [207] H. Abreu et al. (FASER), Eur. Phys. J. C **80**, 61 (2020), 1908.02310.
- [208] C. Ahdida et al. (SHiP) (2020), 2002.08722.
- [209] F. Kling (2020), 2005.03594.
- [210] P. Coloma, P. A. Machado, I. Martinez-Soler, and I. M. Shoemaker, Phys. Rev. Lett. **119**, 201804 (2017), 1707.08573.

- [211] P. Coloma, Eur. Phys. J. C **79**, 748 (2019), 1906.02106.
- [212] C. A. Argüelles, V. Brdar, and J. Kopp, Phys. Rev. **D99**, 043012 (2019), 1605.00654.
- [213] C. T. Kullenberg et al. (NOMAD), Phys. Lett. **B706**, 268 (2012), 1111.3713.
- [214] D. Akimov et al. (COHERENT), Science **357**, 1123 (2017), 1708.01294.
- [215] D. S. M. Alves and N. Weiner, JHEP **07**, 092 (2018), 1710.03764.
- [216] S. Knapen, T. Lin, and K. M. Zurek, Phys. Rev. D **96**, 115021 (2017), 1709.07882.
- [217] A. Anastasi et al., Phys. Lett. B **750**, 633 (2015), 1509.00740.
- [218] J. Bjorken, S. Ecklund, W. Nelson, A. Abashian, C. Church, B. Lu, L. Mo, T. Nunamaker, and P. Rassmann, Phys. Rev. D **38**, 3375 (1988).
- [219] E. Riordan et al., Phys. Rev. Lett. **59**, 755 (1987).
- [220] M. Davier and H. Nguyen Ngoc, Phys. Lett. B **229**, 150 (1989).
- [221] M. Battaglieri et al., Nucl. Instrum. Meth. A **777**, 91 (2015), 1406.6115.
- [222] J. Grange et al. (Muon g-2) (2015), 1501.06858.
- [223] M. Abe et al., PTEP **2019**, 053C02 (2019), 1901.03047.
- [224] G. Abbiendi et al., Eur. Phys. J. C **77**, 139 (2017), 1609.08987.
- [225] J. Lees et al. (BaBar) (2020), 2005.01885.
- [226] L. Lavoura, Eur. Phys. J. C **29**, 191 (2003), hep-ph/0302221.
- [227] A. M. Sirunyan et al. (CMS), JHEP **11**, 151 (2018), 1807.02048.
- [228] G. Aad et al. (ATLAS), JHEP **10**, 096 (2014), 1407.0350.
- [229] A. M. Sirunyan et al. (CMS), Phys. Lett. B **790**, 140 (2019), 1806.05264.
- [230] K. Babu, P. B. Dev, S. Jana, and A. Thapa, JHEP **03**, 006 (2020), 1907.09498.
- [231] G. Funk, D. O’Neil, and R. Winters, Int. J. Mod. Phys. A **27**, 1250021 (2012), 1110.3812.
- [232] W. Grimus, L. Lavoura, O. Ogreid, and P. Osland, J. Phys. G **35**, 075001 (2008), 0711.4022.
- [233] W. Grimus, L. Lavoura, O. Ogreid, and P. Osland, Nucl. Phys. B **801**, 81 (2008), 0802.4353.
- [234] A. W. El Kaffas, W. Khater, O. M. Ogreid, and P. Osland, Nucl. Phys. B **775**, 45 (2007), hep-ph/0605142.